High-fidelity simulations and data-driven insights on rate-governing phases in duplex and triplex systems during isotropic normal grain growth

P. G. Kubendran Amos [1,2,*] Arnd Koeppe,[2,3] Ramanathan Perumal,[2,3] and Britta Nestler[2,3]

[1]*Theoretical Metallurgy Group, Department of Metallurgical and Materials Engineering,*
National Institute of Technology, Tiruchirappalli 620015, Tamil Nadu, India

[2]*Institute of Applied Materials (IAM-MMS), Karlsruhe Institute of Technology (KIT), Strasse am Forum 7, 76131 Karlsruhe, Germany*

[3]*Institute of Digital Materials Science (IDM), Karlsruhe University of Applied Sciences, Moltkestr. 30, 76133 Karlsruhe, Germany*

Normal grain growth in multiphase polycrystalline systems includes sluggish evolution of minor-phase grains and relatively faster growth of the major-phase grains. Which of these two factors predominantly affects the growth kinetics of the overall microstructure remains an open question. Critical insights to answer this question are offered in this work, through data science techniques, by cumulatively analyzing the influence of the evolution rate of all constituent phase grains on the simulated growth kinetics of duplex and triplex microstructures. Moreover, predictive models relating volume fraction of the constituent phases to the growth kinetics of multiphase systems are developed and are extensively validated. The simulated data set encompassing a large area of interest and feature-rich information, which lends itself to the current analyses, is built through a suitable data-acquisition strategy, and a thermodynamically consistent multiphase-field approach. Statistical analyses of 14 triplex and 5 duplex microstructures, included in the data set, unravel that the grain-growth kinetics in both multiphase systems is primarily governed by the evolution rate of phase(s) occupying larger volume fraction. This effect is observed in spite of the sluggish growth exhibited by the minor-phase grains. Furthermore, the predictive models, developed using regression and feed-forward neural network, indicate a nonlinear, but proportional, relation between the phase fractions and kinetic coefficients that quantify the grain-growth rate of multiphase systems.

I. INTRODUCTION

A. Multiphase polycrystalline materials

Microstructures of materials are meticulously engineered to cater to ever demanding needs of technological progress. Properties, once thought to be irreconcilable, are increasingly combined through appropriate combination of phases in microstructures [1–3]. Even though microstructures characterized by more than one chemically distinct phase have been around for a considerable period of time, the distribution of the constituent phases engenders a unique category of multiphase materials. For instance, in polycrystalline pearlitic steel, the combination of ferrite and cementite in a specific phase fraction is observed in all grains, despite being separated by the interfaces (grain boundaries) [4,5]. Such grains can be treated as chemically homogeneous, despite the presence of two distinct phases. However, on the other hand, there are specialized steels, wherein the grains are not chemically homogeneous but are exclusively associated with the constituent phases [6]. In other words, instead of martensite and ferrite coexisting in all grains of the polycrystalline microstructure, individual grains assume a specific phase, thereby establishing a chemical inhomogeneity in the system [7]. Polycrystalline materials, characterized by these chemically distinct grains,

are qualified contextually as multiphase, and depending on the number of constituent phases, these materials are referred to as duplex, triplex, and such.

Aside from steel, multiphase microstructures are established in a wide range of materials to achieve a desired combination of properties [8,9]. The extensive applicability of two- and three-phase titanium alloys is primarily due to properties which is a direct consequence of their multiphase microstructure. The prevalence of multiphase polycrystalline arrangement in high-entropy alloys is a principal reason for their characteristic behavior [10,11]. In ceramics, mechanical properties including fracture toughness are noticeably enhanced by a two-phase microstructure. The duplex system of alumina and silicon carbide is a prime example of such behavior-enhanced ceramics [12,13]. Moreover, it has been reported that the introduction of an additional phase, which institutes a triplex microstructure, exacts a more preferred response from ceramics to an imposed mechanical condition [14,15]. Similar favorable effects of multiphase microstructure are observed in composite materials as well [16].

B. Grain growth in multiphase microstructures

Properties of the multiphase materials, in addition to the characteristic features of the constituent phases, are noticeably influenced by microstructural features that primarily include the average grain size and volume fraction of the

*Corresponding author: prince@nitt.edu

phase, i.e., phase fraction. Consequently, to achieve desired behavior, multiphase materials with appropriate grain sizes and varying phase fraction ranging from minimal minor phase (close to 1%) to equifraction (50-50 in duplex) are fabricated [17,18]. While material-specific processing techniques are employed for introducing the necessary phase fraction, the required grain sizes are rather obtained through a well-known microstructural transformation called grain growth [19]. The mechanism of grain growth in multiphase systems is significantly different from single-phase polycrystalline microstructure. In polycrystalline materials with chemically homogeneous grains, the local diffusion of atoms across the grain boundaries, which consequently leads to its migration, ultimately governs the grain growth. In other words, the grain growth in single-phase systems is primarily dictated by the movement of the interface (or) grain boundaries. However, in multiphase microstructures, the association of grains to a specific constituent phase adds an additional facet to the conventional grain growth. Aside from reducing the number of grains, grain growth in multiphase systems conserves the characteristic volume fraction of the phases. Therefore, the curvature-driven transformation, which minimizes the overall grain-boundary energy, in multiphase materials is, in principle, a combination of coarsening and grain growth [20]. Typifying features of both coarsening and grain growth, which respectively are preservation of volume fraction and growth of larger grains at the expense of smaller ones, are simultaneously observed in multiphase materials. For this reason, the energy-minimizing curvature-driven transformation in multiphase systems is, at times, referred to as concurrent grain growth and coarsening. Correspondingly, as opposed to interface migration, the long-range diffusion of atoms dictates grain growth in multiphase polycrystalline systems [21]. Regardless of the mechanism, owing to the influence of the grain size on the properties rendered by the materials, grain growth in multiphase systems has been extensively analyzed [22,23]. Moreover, it is conceivable, and indeed reported, that a change in the average grain size of a multiphase material, while employed in an application, results in undesired behavior. In other words, aside from the direct effect of grain size on the properties of multiphase materials, its life in an application is dictated by the rate at which the grains grow. Solid-oxide fuels with triplex microstructure are prime examples of this relation between the growth kinetics and life of a material [24]. Considering this influence of grain size, investigations have been geared towards understanding the kinetics of grain growth in multiphase polycrystalline system.

C. Focusing on generalized features

Experimental techniques generally pose definite practical difficulties when adopted for comprehensive analyses of grain growth. Therefore, theoretical approaches have long since been adopted to complement, and extend, the existing understanding [25–27]. These theoretical studies, particularly ones involving multiphase-field models, have been offering critical insights on mechanism and kinetics of grain growth in multiphase system, which are consistent with the experimental observation [28–30]. Existing investigations, and

resulting understanding, of grain-growth kinetics in multiphase polycrystalline systems can broadly be categorized into two. One relates material-specific parameters, including diffusivities and grain-boundary energy anisotropies, to the rate of grain growth [31,32], while the other focuses on the effect of microstructural features like phase fractions [18,33]. The material-specific studies are, in principle, inherently bound by the choice parameter(s). On the other hand, the analyses involving phase fraction offer more generalized insights that are relevant to a wide range of multiphase polycrystalline systems.

In keeping with the change in grain-growth mechanism, the investigations focusing on microstructural features unravel that the introduction of second phases significantly reduces the kinetics of overall evolution. Moreover, it is realized that the expression capturing the temporal change in the average radius of the polycrystalline system reflects coarsening kinetics, $\bar{R}^n \propto t$ with $n = 3$, irrespective of the volume fraction of the second phase [21,34]. Even though the major and minor phases, categorized based on volume fraction, and the entire polycrystalline system as a whole, evolve at a rate that complies with the coarsening power law, the kinetic coefficients (k) vary between the phases based on their volumes [18]. For instance, in a duplex microstructure characterized by unequal volume fraction of constituent phases, the grains of the major phase, with higher phase fraction, grow at the noticeably faster rate when compared to the minor phase. This disparity in the kinetics of the grain growth between the phases is indicated by the difference in the kinetic coefficient (k). The relatively sluggish growth of the minor phase(s) is attributed to the increased distance between the respective chemically similar grains, and complex diffusion pathways that facilitate the growth, when compared to the proximity of the major phases. Furthermore, attempts have been made to quantify the effect of volume fraction on the kinetic coefficients of major and minor phases by comparing the evolution of the microstructures with varying phase fractions [33]. In the above and subsequent discussions, it is vital to note that the terminologies minor and major phase are subjectively used. Therefore, a given phase, in the context of a specific multiphase microstructure, might assume a role of a minor phase, whereas in other systems, it would be treated as a major constituent.

Despite the advancements, there continues to exist certain aspects to the grain-growth kinetics that prevent a comprehensive understanding of the evolution of multiphase polycrystalline systems. For instance, studies aimed at explicating the grain-growth rate in multiphase materials primarily report, and discuss, on the difference in the kinetics exhibited by the major and minor phases, while largely overlooking the evolution of the entire microstructure [12,35]. Moreover, the collective influence of the growth rate of major and minor phases on the temporal change in overall average size of the grains is yet to be convincingly understood. In three (or more) phase systems, particularly, the interdependency between the grain-growth rate of different phases has not been considered in depth so far. Amongst others, in this work, a step is taken towards addressing the aforementioned questions on the grain-growth kinetics of the overall multiphase microstructure through appropriate statistical analysis.

II. ACQUIRING INFORMATION-RICH DATA SET

Persuasive understanding on the relation between the evolution of individual phase grains and the overall grain growth in a multiphase system demands a systematic approach that renders the feature-rich information. To that end, a "multidimensional" data set is developed by modeling grain growth exhibited by duplex and triplex microstructures in the multiphase-field framework [36,37]. Thermodynamic underpinnings of the adopted model are rather well established, and is often presented as a computationally efficient alternate [38,39]. Even though the complete formulation of the present approach [40,41], its ability to incorporate different modes of mass transfer, and recover sharp-interface solutions is exhaustively discussed elsewhere [42,43], a brief outline focusing on the key aspects is rendered here. Moreover, the terms associated with the governing expressions are delineated in Appendix A.

A. Multicomponent multiphase-field model

The multiphase-field approach is characterized by the introduction of scalar variable(s) which distinguishes the different phases in the system. Conventionally, while modeling polycrystalline microstructures, these variables, called phase field $[\phi(x, t)]$, are employed to differentiate various grains, and their spatiotemporal evolution translates to grain growth. Across the grain boundary separating two grains, phase field assumes a value of $\phi = 0$ in one grain, while the other is realized by a constant nonzero value, which is generally $\phi = 1$. The diffuse region, wherein the value of the phase field gradually varies, $\phi(x, t) \in (0, 1)$, describes the grain boundary. Given that, in most cases, the grains in the polycrystalline systems are chemically homogeneous, phase field typifying the various grains are introduced as a tuple, which is expressed as

$$\boldsymbol{\phi} = \{\phi_1, \phi_2, \ldots, \phi_N\}, \tag{1}$$

where N denotes the total number of grains in the system. However, since the present approach models grain growth in multiphase systems comprising of N phases, wherein numerous grains are associated each phase, the corresponding phase field is extended and written as

$$\boldsymbol{\phi} = \left\{ \underbrace{\{\phi_\alpha^1, \phi_\alpha^2 \ldots \phi_\alpha^{q_\alpha}\}}_{\boldsymbol{\phi}_\alpha}, \underbrace{\{\phi_\beta^1, \phi_\beta^2 \ldots \phi_\beta^{q_\beta}\}}_{\boldsymbol{\phi}_\beta} \ldots \underbrace{\{\phi_N^1, \phi_N^2 \ldots \phi_N^{q_N}\}}_{\boldsymbol{\phi}_N} \right\}. \tag{2}$$

Moreover, in this formulation, number of grains sharing a given phase is represented by q_i where $i \in \{\alpha, \beta, \ldots, N\}$. By assigning appropriate concentration, grains of a given phase are distinguished from the rest, $\{\boldsymbol{\phi}(c) = \boldsymbol{\phi}_\alpha(c) | c = c_\alpha\}$.

Similar to phase field, in order to encompass the K-different chemical components, the concentration is introduced as a tuple. Correspondingly, concentration of a random grain m associated with phase α reads as

$$\boldsymbol{c}_m^\alpha = \left\{ c_{m:i}^\alpha, c_{m:j}^\alpha, \ldots, c_{m:K}^\alpha \right\}. \tag{3}$$

The homogeneity in the chemical composition of the grains associated with a given phase, say α, yields

$$\boldsymbol{c}_1^\alpha = \cdots = \boldsymbol{c}_m^\alpha = \cdots = \boldsymbol{c}_{q_\alpha}^\alpha \equiv \boldsymbol{c}^\alpha = \left\{ c_i^\alpha, c_j^\alpha, \ldots, c_k^\alpha \right\}. \tag{4}$$

To ensure that the volume fraction of the phases remains unaltered despite the evolution, equilibrium composition is assigned to the corresponding phases. In other words, since the current approach attempts to model grain growth in a multiphase system, $\boldsymbol{c}^\alpha$ represents a tuple of equilibrium composition that characterizes phase α.

Following the conventional framework, the overall energy density of the multiphase polycrystalline system is formulated as the combination interface (grain boundaries) and bulk (grain) contribution [44]. Correspondingly, by incorporating the appropriate phase field and concentration, the energy density of the system comprising of N phases and K chemical components is written as

$$\mathcal{F}(\boldsymbol{\phi}, \boldsymbol{\nabla\phi}, \boldsymbol{c}) = \mathcal{F}_{\text{int}}(\boldsymbol{\phi}, \boldsymbol{\nabla\phi}) + \mathcal{F}_{\text{bulk}}(\boldsymbol{\phi}, \boldsymbol{c})$$
$$= \int_V f_{\text{int}}(\boldsymbol{\phi}, \boldsymbol{\nabla\phi}) + f_{\text{bulk}}(\boldsymbol{\phi}, \boldsymbol{c}) dV, \tag{5}$$

where $f_{\text{bulk}}(\boldsymbol{\phi}, \boldsymbol{c})$ and $f_{\text{int}}(\boldsymbol{\phi}, \boldsymbol{\nabla\phi})$ are the respective energy contribution of grain and grain boundary with V representing the volume of the entire domain. The interface contribution $f_{\text{int}}(\boldsymbol{\phi}, \boldsymbol{\nabla\phi})$, akin to most multiphase-field techniques, comprises of a gradient and potential-energy term. Grain-boundary energy densities, and corresponding anisotropies, are introduced to the system through the interface-energy contribution [45]. While multiwell potentials are generally employed to penalize phase field and ensure its bounds, in this work, an obstacle-type potential operating in combination with Gibbs simplex is involved [46]. Furthermore, the energy contributions from the grains $f_{\text{bulk}}(\boldsymbol{\phi}, \boldsymbol{c})$, which is reasonably assumed to be insignificant while modeling grain growth in a single-phase system, is formulated as the interpolation of the energy contribution of the individual grains, $f(\boldsymbol{\phi}, \boldsymbol{c}) = \sum_\alpha^N \sum_m^{q_\alpha} f_m^\alpha(\boldsymbol{c}^\alpha) h(\phi_\alpha^m)$. Given that the contribution of the individual grains is dictated by the characteristic equilibrium composition of the associated phases, the volume of the phases during grain growth is preserved by the energy-density term $f_{\text{bulk}}(\boldsymbol{\phi}, \boldsymbol{c})$ [47,48].

The spatiotemporal evolution of phase field, which translates to grain growth, is formulated by considering phenomenological minimization of the overall energy density of the system. Correspondingly, the evolution of a random grain m, which is associated with phase α, is dictated by

$$\tau\varepsilon\frac{\partial\phi_\alpha^m}{\partial t} = -\frac{\partial\mathcal{F}(\boldsymbol{\phi}, \boldsymbol{\nabla\phi}, \boldsymbol{c})}{\partial\phi_\alpha^m} = \varepsilon\left[\boldsymbol{\nabla}\cdot\frac{\partial a(\boldsymbol{\phi}, \boldsymbol{\nabla\phi})}{\partial\boldsymbol{\nabla}\phi_\alpha^m} - \frac{\partial a(\boldsymbol{\phi}, \boldsymbol{\nabla\phi})}{\partial\phi_\alpha^m}\right] - \frac{1}{\varepsilon}\left[\frac{\partial w(\boldsymbol{\phi})}{\partial\phi_\alpha^m}\right] - \left[\frac{\partial f_m^\alpha(\boldsymbol{c}^\alpha, \phi_\alpha^m)}{\partial\phi_\alpha^m}\right] - \Lambda, \tag{6}$$

where the Lagrange multiplier Λ is introduced to ensure that the summation of phase fields at any point, and time, in the system is 1. Moreover, in the above evolution equation, while $a(\boldsymbol{\phi}, \boldsymbol{\nabla\phi})$ and $w(\boldsymbol{\phi})$ correspond to the gradient and potential energy terms, the parameter dictating interface width, and its stability during the migration, are denoted by ε and τ, respectively.

TABLE I. Equilibrium concentration of binary and ternary systems in mole fraction.

Phase	Independent component i	Independent component j
(Binary)		
Phase α	0.1	
Phase β	0.9	
(Ternary)		
Phase α	0.05	0.05
Phase β	0.05	0.9
Phase γ	0.9	0.05

In multiphase-field models, wherein the energy contribution of the bulk phases is described based on the dependent concentration, the corresponding driving force, which emerges from $\frac{f_m^\alpha(\mathbf{C}^\alpha, \phi_\alpha^m)}{\partial \phi_\alpha^m}$ in Eq. (6), and dictates the evolution of phase field, can be viewed as the difference in the Legendre transform of the free-energy densities. This understanding forms the basis of the grand-potential approach, and when consistently extended assumes chemical potential as the continuous and dynamic variable replacing phase-dependent concentration [49]. Given its computational efficiency, this approach is adopted in this work, and the driving force dictating phase-field evolution is formulated by treating chemical potential as the dynamic variable. The temporal evolution of the chemical potential, which principally governs the bulk driving force in phase-field evolution, is written as

$$\frac{\partial \mu_i}{\partial t} = \left\{ \nabla \cdot \left[\sum_{j=1}^{K-1} \mathbf{M}(\boldsymbol{\phi}) \nabla \mu_j \right] - \sum_\alpha^N \sum_m^q c_i^\alpha \frac{\partial \phi_\alpha^m}{\partial t} \right\} \left[\sum_\alpha^N \sum_m^q h(\phi_\alpha^m) \frac{\partial c_{m:i}^\alpha}{\partial \mu_j} \right]_{ij}^{-1}, \tag{7}$$

where μ_i denotes the continuous chemical potential of component i. The mobility of the migrating elements, in the multicomponent setup, is dictated by matrix $\mathbf{M}(\boldsymbol{\phi})$ which also facilitates the incorporation of surface diffusion [42,43]. The phase-dependent concentration of component i in random grain m belonging to phase α, and the corresponding interpolation function, are represented by $c_{m:i}^\alpha$ and $h(\phi_\alpha^m)$, respectively. The evolution of the different microstructures with varying phase fractions, in this work, is modeled by solving Eqs. (6) and (7).

Although Eq. (7) delineates the evolution of chemical (diffusion) potential, the associated expression, as discussed in Appendix A, is essentially derived from the temporal change in the concentration. In this work, the phase fraction of the multiphase polycrystalline systems is preserved by associating the phases with the respective equilibrium concentration. These equilibrium concentrations are listed in Table I. In addition to establishing chemical equilibrium, assigning specific concentration to the grains associates them to particular phases. The equilibrium established through the concentration gets locally disturbed by the difference in the curvature of the grains ($\mathbf{K}$) resulting from their sizes and topological factors. The curvature difference ultimately leads to the flux of solute from the smaller to larger grains of a given phase. This migration of concentration fundamentally, driven by the curvature difference, introduces grain growth similar to that of coarsening, wherein despite the decrease in the number of grains, the volume fraction of the phases is largely conserved.

B. Simulation setup

Existing studies unravel that, unlike Zener pinning [50], the overall trend in grain-growth kinetics exhibited by the individual phases, and entire microstructure, of the multiphase system is largely independent of the dimensionality of the simulation domain [18,33,51]. In other words, similar disparity in the evolution kinetics of major, minor, and equifraction phases, in relation to overall growth rate, has been reported for both two- and three-dimensional setups. Therefore, in this work, the grain growth in various multiphase-polycrystalline systems is modeled in a two-dimensional framework.

Irrespective of the phase fraction, all the two-dimensional domains considered in the present investigation share identical configurations. Polycrystalline microstructures comprising of approximately 10 000 grains are established over the discretized domain through Voronoi tessellation. These two-dimensional domains are uniformly discretized into 2048 × 2048 cells of size, $\Delta x = \Delta y = 5 \times 10^{-7}$ m, through the finite-difference scheme.

The grains are associated to the constituent phases by assigning the characteristic chemical composition. Given that the principal focus of this work is to understand the evolution kinetics of different phases in relation to each other, and to the overall grain-growth rate, a rather straightforward distinction is made between the phases. While a binary system with two chemical components $\tilde{i}$ and $\tilde{j}$ is considered for establishing duplex microstructure, a three-phase microstructure is construed in the framework of ternary system with components $\tilde{i}$, $\tilde{j}$, and $\tilde{k}$. In a duplex system, α phase is an $\tilde{i}$-rich phase with equilibrium composition of $c_{\tilde{i}:eq}^\alpha = 0.9$, and $c_{\tilde{j}:eq}^\gamma = 0.9$ characterizes matrix γ phase, wherein both concentrations are expressed in mole fraction. Concentration of the solvent in α and γ phases remains unaltered in the triplex system, while the remnant content is equally partitioned between solutes $\{\tilde{j}, \tilde{k}\}$ and $\{\tilde{i}, \tilde{k}\}$, respectively. The β phase, exclusively introduced in the three-phase systems, is characterized by composition $c_{\tilde{i}:eq}^\beta = c_{\tilde{j}:eq}^\beta = 0.05$.

Since the grains are equiaxed with almost similar size, the required phase fraction in the microstructure is achieved by relating the appropriate number of randomly distributed

TABLE II. System-specific parameters.

Parameter	Symbol	Value
Grain boundary energy	$\bar{\gamma}_{\alpha\alpha} = \bar{\gamma}_{\beta\beta}\bar{\gamma}_{\gamma\gamma}$	$1.0 \, \text{Jm}^2$
Interphase boundary energy	$\bar{\gamma}_{\alpha\beta} = \bar{\gamma}_{\beta\gamma} = \bar{\gamma}_{\alpha\gamma}$	$1.0 \, \text{Jm}^2$
Bulk diffusivities	$D^\alpha = D^\beta = D^\gamma$	$1.0 \, \text{m}^2\text{s}^{-1}$

grains to the corresponding phases. In other words, duplex microstructure comprising of 33% minor phase is devised, in the initial stages, by assigning the respective chemical composition to one-third of the grains randomly.

Material-specific parameters, including grain boundary energy, and simulation parameters involved in the present analysis are presented in Tables II and III, respectively. Reflecting the isotropic nature of the microstructure, identical energies are assigned for grain and interphase boundaries. Furthermore, it is assumed that the components diffuse at a constant rate irrespective of the phases. Although these considerations can reasonably be deemed as unphysical, they facilitate in efficiently realizing the effect of phase fractions on the overall grain-growth kinetics exhibited by the multiphase systems. Stated otherwise, the rather straightforward treatment of the material parameters lends itself to the exclusive focus on understanding the evolution rate of the polycrystalline with respect to the growth kinetics of individual phases.

The temporal evolution of the dynamic variables, phase field, and chemical potential, that dictate the microstructural changes in the multiphase polycrystalline system, are solved over the homogeneous cells of the two-dimensional domain by forward-marching Euler's scheme. In order to ensure that the computational resources are optimally used, the domain is decomposed into smaller segments, and dealt simultaneously through message passing interface (MPI).

C. Homogeneous and multiphase microstructures

In applications, depending on the material need, multiphase systems with varying degrees of phase fractions are employed. Although investigating every combination of the phase fraction would be redundant, convincing level of understanding can only be gained by systematically capturing the entire area of interest in the *space* of different phase fractions. Particularly, since this study adopts statistical techniques to explicate the kinetic relation between the evolving phases, the performance of the predictor depends on the wealth of information in the data. To that end, in this work, grain growth in 20 different systems, which encompasses 1 homogeneous single-phase, 5 duplex, and 14 triplex microstructures, is mod-

TABLE III. Simulation parameters.

Parameter	Symbol	Value
Time-step width (No unit [42])	Δt	1.0
Interface-width parameter	ε	0.2 μm [52]
Relaxation parameter	τ	$1.0 \, \text{Jsm}^{-4}$

eled, and "multidimensional" data set is built by monitoring the temporal evolution of the grains.

As opposed to random consideration of different volume fractions of phases, a systematic choice of various phase fraction is made from a 2-simplex design space. The simplex, in its entirety, along with the section focused for the current study, is shown in Fig. 1(a). The points within, and on, the 2-simplex can be interpreted in a manner akin to the ternary isotherm. Correspondingly, while the three vertices indicate the homogeneous microstructure of phases α, β, and γ, the duplex microstructures are encapsulated by the edges joining the vertices. Any point within the simplex represents triplex system, with phase fraction dictated by its position. As illustrated in Fig. 1(a), a section of the simplex emanating from the vertex characterizing the homogeneous γ microstructure is considered for the present analyses. This section of the simplex renders a wide variety of polycrystalline systems ranging from single-phase homogeneous to triplex with equifraction of constituent phases. Moreover, owing to the configuration of the section in Fig. 1(a), the γ phase acts as the matrix for the duplex and triplex microstructures with unequal volume fractions of phases. Multiphase microstructures corresponding to the different points of the simplex section are collectively illustrated in Fig. 1(b). Although the volume fraction of the minor phases can be as low as 5%, the grains associated with these phases hardly occupy a position on the grain boundary. In other words, despite the low volume fraction and reduced size, the grains of the minor phases seldom render an influence analogous to the particles in Zener pinning. Moreover, the reduced size of the grains associated with minor phases, in the initial stages of the grain growth, is consistent with experimental observations [23,53,54] and existing theoretical studies [18,33].

III. RESULTS AND DISCUSSION

By monitoring the grain growth exhibited by the homogeneous and multiphase systems, a multidimensional data set is devised which essentially comprises of a temporal change in the average radius of the individual phase-associated grains, and the entire microstructure as a whole. This data set is analyzed through established and robust statistical techniques to unravel the effect of the individual phases on the evolution kinetics of the entire system. Moreover, a cross-validation strategy is adopted to further increase the rigor of the models and to evaluate their performance against unknown data not used for training.

A. Duplex microstructures

A duplex microstructure comprises of two distinct phases, and is characterized by grains associated with one of these constituent phases α and γ. Despite the inhomogeneity in the concentration distribution, in duplex microstructures, given that the grain growth occurs in a continuum, the temporal evolution of one phase, and its corresponding kinetics, is inherently coupled with the other. This is illustrated and discussed in Appendix C. In other words, the growth rate exhibited by the duplex microstructures with varying phase fractions can be convincingly expressed by considering
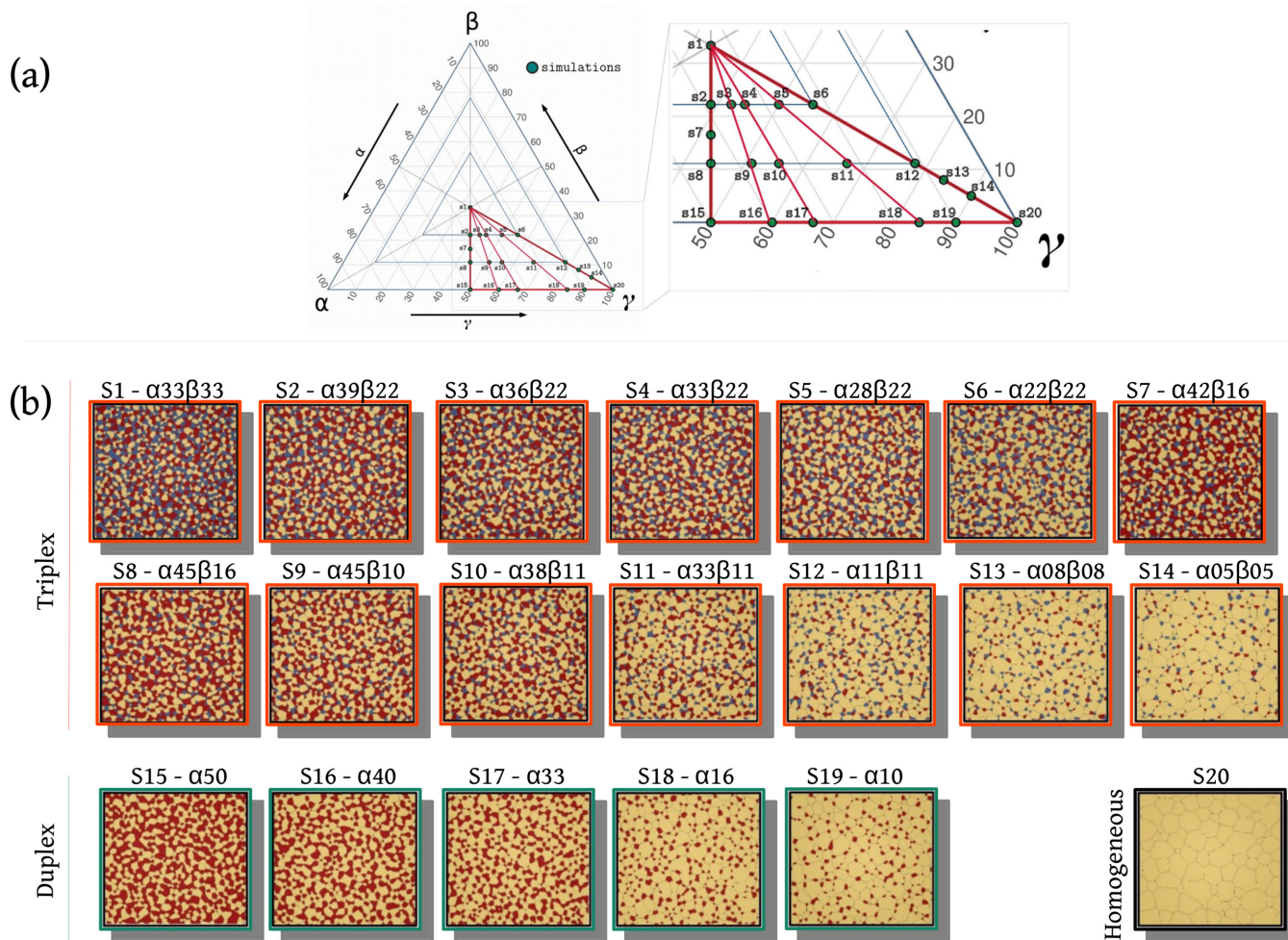
FIG. 1. (a) A simplex, analogous to ternary isotherm, depicting all-possible phase fractions in duplex and triplex microstructures, along with single-phase systems (vertices). The section that encompasses the varied microstructures considered in this work is distinguished, and each point referring to a specific system is highlighted and designated as $S1$, $S2$, and such. (b) Microstructure corresponding to each point in the section of the simplex that includes homogeneous systems along with duplex and triplex microstructures with varying volume fraction of the constituent phases. The name Si, where i would vary from 1 to 20, assigned every microstructure facilitates in relating the corresponding phase fraction to the specific in the simplex.

kinetics of the only one of the evolving phases. Therefore, the aim of the present investigation in duplex microstructure reduces to identifying which of the phases, major or minor, principally governs the kinetics of overall grain growth.

1. Preliminary validating investigations

Before proceeding to realize the degree of influence rendered by the different phases on the overall growth kinetics exhibited by the duplex microstructure, conventional investigations are pursued to verify the outcomes of the present approach in relation to the existing reports [18,21]. In Fig. 2, the progressive change in the average radius of homogeneous and two duplex microstructures with time is presented. Moreover, the temporal increase in the average radius of the phase-associated grains is monitored, and included in this illustration. While $\bar{R}(t)$ represents the average radius of the entire polycrystalline microstructure, the corresponding parameter for the grains of phases α and γ in duplex microstructures is, respectively, denoted by $\bar{R}_\alpha(t)$ and $\bar{R}_\gamma(t)$.

Moreover, the multiphase microstructures in this, and subsequent, discussions are described based on the volume fraction of the minor phase. For instance, $\alpha10$ indicates duplex microstructure with 10% phase α, while the equifraction system is denoted $\alpha50$.

With the introduction of a second phase in the microstructure, in Fig. 2, a significant decrease is observed in the rate at which the radius increases with time. This noticeable change in the kinetics is predominantly due to the change in grain-growth mechanism, which is governed by the long-range diffusion of the chemical components in duplex microstructure. Moreover, in a system with equal volume fraction of phases, the temporal increase in average radius of the entire microstructure and individual phases is largely identical with marginal deviation. On the other hand, in $\alpha10$, significant disparity is noticed in the rate at which the major-phase grains evolve when compared to the minor phase. Figure 2 illustrates that the increase in the average radius of the entire duplex microstructure lies in-between the growth exhibited by the individual phases. The difference on the growth kinetics
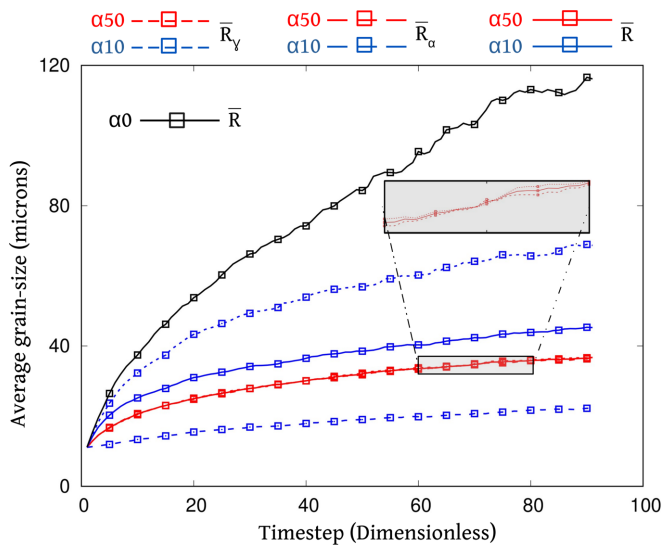
FIG. 2. Temporal change in the average radius of the phase α and γ grains, $\bar{R}_\alpha(t)$ and $\bar{R}_\gamma(t)$, and the entire microstructure $\bar{R}(t)$ for homogeneous and duplex systems characterized by 50% and 10% of phase α. Section of the curves indicating the evolution of average grain sizes in equifraction system is zoom-in to reveal the closeness of growth kinetics exhibited by individual phases and the overall microstructure.

between the phases, exclusively in the duplex microstructure characterized by unequal volume fraction, is due to the corresponding distribution of the phases. Owing to its reduced volume, the grains of the minor phase in $\alpha10$ microstructure are considerably separated when compared to major-phase grains. Therefore, the diffusion path, which the chemical components need to transverse to achieve grain growth, is longer and more convoluted. Consequently, the growth rate exhibited by the minor-phase grains is significantly lower than the grains of phase γ.

2. Grain-growth kinetics

Even though the kinetics illustrated in Fig. 2 renders a progressive increase in the average radius with time, owing to the difference in the governing mechanism, the exponent of the power law capturing the growth kinetics varies depending on the nature of the system [18,21]. While the exponent $n = 2$ characterizes grain growth in a homogeneous system, evolution kinetics of the individual phases, and the duplex microstructure as a whole, largely follow relation $\bar{R}^3(t) \propto t$. In order to affirm that the evolution of the entire microstructure, and its corresponding phases, adhere to the power law, the temporally varying average radius is raised to different exponents, $n = \{1, 2, 3, 4\}$, and related to time. The correlation coefficient (Pearson) characterizing the relation between the average radius with the various exponents and time is ascertained, and graphically represented in Fig. 3. In this illustration, $\langle \bar{R}^n, t \rangle$ denotes the correlation coefficient between the average radius raised to order n and time. Figure 3 shows that, in homogeneous system ($\alpha0$), maximum correlation is observed when $n = 2$, thereby indicating that the grain growth in this microstructure adheres to the power law $\bar{R}^2(t) \propto t$. Furthermore, correlation coefficient relating the average radius of
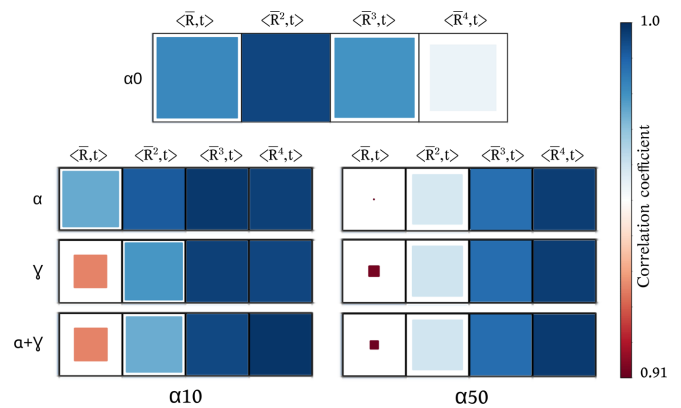

FIG. 3. Correlation coefficient characterizing the proportionality between time and the average radius of individual phase grains and entire microstructure, raised to different exponents, for homogeneous and duplex systems $\alpha50$ and $\alpha10$.

the individual phases, and entire duplex microstructures, with time, is higher when $n = 3$, which implies that the evolution in the multiphase systems complies to the established power law [21]. Even though it might appear that, in Fig. 3, for equifraction duplex system ($\alpha50$), the maximum correlation is observed in $n = 4$, given the marginal difference when compared to $n = 3$, such consideration leads to *overfitting*, thus returning to $\bar{R}^3(t) \propto t$ as the statistically sound relation. A brief discussion on realizing overfitting is presented in Appendix B.

The preliminary studies and their corresponding outcomes, as selectively illustrated in Fig. 3, indicate a microstructural evolution induced in the multiphase polycrystalline system, in spite of the chemical equilibrium established between the phases through appropriate compositions. Moreover, it is evident from Fig. 3 that the kinetics associated with this evolution adheres to a power law generally associated with coarsening, which is principally driven by curvature difference through the long-range diffusion of the chemical species. Therefore, though the chemically distinct phases in a multiphase polycrystalline system introduce a characteristic change in the kinetics of grain growth, the discernible increase in average radius affirms that the evolution remains fundamentally governed by the curvature difference, wherein the larger grains grow at the expense of the smaller ones. Despite being compliant with the well-established understanding and existing reports, these analyses are largely unsuccessful in delineating the evolution kinetics of the entire duplex microstructure in relation to the growth rate of the constituent phase grains. This lack of adequate insight lends itself to the subsequent investigations.

3. Ascertaining governing factor

As opposed to the representative analysis for validation, all duplex microstructures indicated in Fig. 1 are statistically analyzed to realize the relative influence of the evolving major- and minor-phase grains on the overall grain-growth kinetics. Correspondingly, both R and Python with the TENSORFLOW [55] and CIDS [56] libraries are employed for the

statistical evaluation. The project data are managed by Kadi through the Python interface (Kadi4mat) [57].

From the data set comprising of temporally varying average radius, the growth rate exhibited by the individual phase grains ($d\bar{R}_\alpha/dt$ or $d\bar{R}_\gamma/dt$) and entire microstructure ($d\bar{R}/dt$), at every instance (t), is determined for each duplex system. Subsequently, by treating the growth rate of the individual phase grains, and entire microstructure, as *response* and *predictor* variable, respectively, the corresponding kinetics are related to each other. From the emerging relation, the *coefficient of determination* χ for the combination of an individual phase grain and overall microstructure is estimated. Scatter plots illustrating the dependency of $d\bar{R}_\alpha/dt$ or $d\bar{R}_\gamma/dt$ and $d\bar{R}/dt$ are included in Appendix D.

For a given duplex system, following the conventional description, the coefficient of determination considering the growth kinetics of minor phase α ($d\bar{R}_\alpha/dt$) and entire microstructure ($d\bar{R}/dt$) is calculated by

$$\chi_\alpha = \frac{\chi_\alpha^{\text{SST}} - \chi_\alpha^{\text{SSE}}}{\chi_\alpha^{\text{SST}}}, \qquad (8)$$

where χ_α^{SST} is estimated by treating the instantaneous growth rate of overall microstructure as univariate parameter, and summing up the squares of the disparity (error) between the individual values and the mean. On the other hand, χ_α^{SSE} represents the sum of the squared differences between the data points and regression line relating the instantaneous kinetics of the α-phase grains and overall duplex microstructure.

Using generic variables, the calculation of SST, sum of squares total (χ^{SST}), can be expressed as

$$\chi^{\text{SST}} = \sum_i (y_i - \bar{y})^2, \qquad (9)$$

where y_i and $\bar{y}$ indicate an actual value and mean of all corresponding data, respectively. Additionally, the sum of square error χ^{SSE} involved in Eq. (8) is estimated by

$$\chi^{\text{SST}} = \sum_i (y_i - \hat{y})^2, \qquad (10)$$

with $\hat{y}$ representing the predicted value based on the fitted hypersurface.

Based on the description of the coefficient of determination in Eq. (8), χ_α can be viewed as a parameter that quantifies the effect of α-phase growth kinetics on the evolution rate of entire microstructure. Therefore, in addition to χ_α, the corresponding parameter that realizes the influence of the major-phase growth kinetics ($d\bar{R}_\gamma/dt$) on the overall evolution rate χ_γ is appropriately determined for all the different duplex microstructures considered in this investigation.

Coefficients of determination separately quantifying the role of $d\bar{R}_\alpha/dt$ and $d\bar{R}_\gamma/dt$ in overall growth rate exhibited by the microstructures χ_α and χ_γ are calculated for different duplex systems with varying phase fractions and plotted in Fig. 4. The variation observed in the coefficients of determination, across the different duplex systems, unravels that the effect of individual phase grains on the overall growth kinetics is primarily dependent on the phase fraction of the microstructure. In a duplex system characterized equal volume fraction of phases, identical coefficients of determination
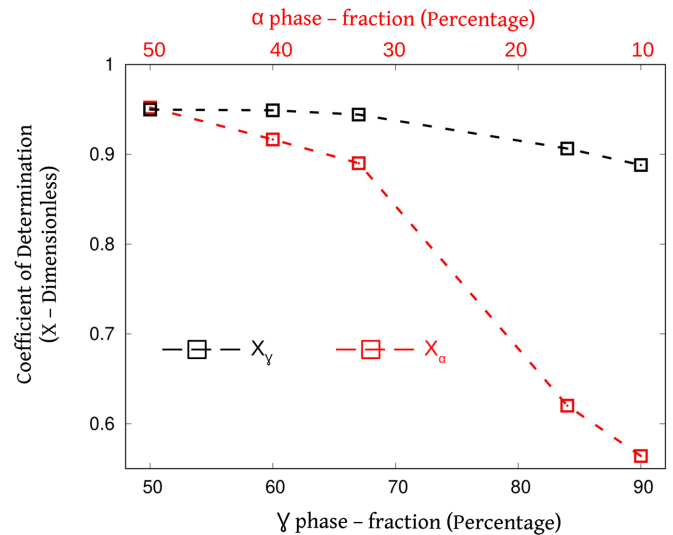

FIG. 4. Coefficient of determination, quantifying the effect of growth kinetics of individual phase grains on the overall grain-growth rate of the entire system, is estimated using Eq. (8) for different duplex microstructures with varying phase fraction.

imply that both α and γ grains similarly influence the evolution kinetics of the entire microstructure. On the other hand, noticeable disparity between χ_α and χ_γ is observed in duplex microstructures with varying volume fraction of constituent phases. Moreover, Fig. 4 shows that this inequality in the coefficients of determination becomes more pronounced with an increase in the difference between the volume fraction of the phases in the duplex microstructure. While the coefficient of determination pertaining to major phase γ exhibits a relatively marginal change, and continues to remain noticeably greater, χ_α progressively decreases with reduction in the volume fraction of the corresponding minor-phase grains. In other words, Fig. 4 unravels that, in duplex systems with unequal volume fraction of phases, the overall growth rate of the entire microstructure ($d\bar{R}/dt$) is primarily influenced by the evolution kinetics of the major-phase grains ($d\bar{R}_\gamma/dt$). Furthermore, it is evident from the illustration that the dominance of the major phase in effecting the overall growth kinetics becomes more definite with increase in the corresponding volume fraction (or decrease in the amount of minor phase).

4. Verifying the statistical claim

In order to substantiate the understanding rendered by the analyses based on coefficient of determination, the temporal change in the average radius of the phase-associated grains ($\bar{R}_\alpha$ or $\bar{R}_\gamma$) and entire microstructure ($\bar{R}$) is studied in a conventional manner. In Fig. 5, the progressive increase in the average radius of major- and minor-phase grains with time, in duplex systems with varying phase fractions, are cumulatively presented. Since the evolution of different duplex microstructures is considered together, for the ease of distinction, temporal change in $\bar{R}_\alpha^3$ and $\bar{R}_\gamma^3$ is adopted for this illustration.

Consistent with the mechanism of evolution, it is observed that the minor-phase grains in system with the minimal volume fraction ($\alpha 10$) grow at a least rate. However, the
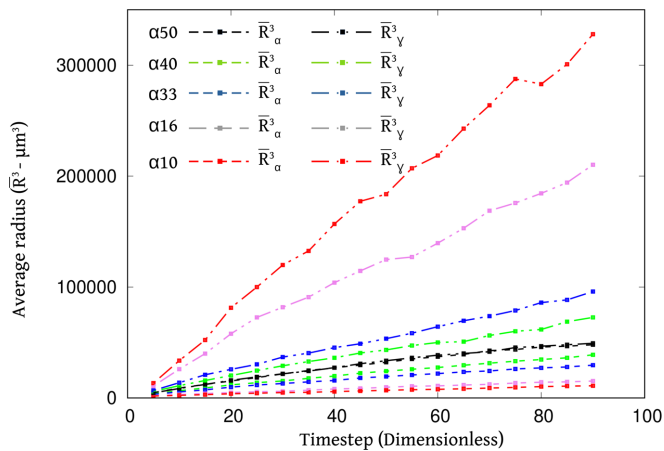
FIG. 5. Progressive increase in the average radius of phase α and γ grains $\bar{R}_\alpha^3$ and $\bar{R}_\gamma^3$, with time for various duplex systems with characteristic phase fraction.

FIG. 6. Temporal change in the average radius of entire duplex systems $\bar{R}^3$ with varying phase fractions during grain growth.

growth kinetics of these grains noticeably increases as the corresponding phase grains occupy more volume in the microstructure. Accordingly, in duplex systems with unequal phase fractions, minor-phase grains of $\alpha40$ microstructure exhibit the highest growth rate, followed by $\alpha33$ and $\alpha16$. On the other hand, the evolution kinetics of major-phase grains is minimal in the $\alpha40$ system, and significantly increases in $\alpha33$ and $\alpha16$ as the volume fraction of the phase α reduces. Moreover, the maximum growth rate in γ-phase grains is observed in microstructure with minimal volume of minor phase $\alpha10$. Owing to the influence of volume fraction, which governs the kinetics through the diffusion paths, the disparity in the temporal change in average radius of the major- and minor-phase grains becomes more evident as the inequality in phase fraction increases. In other words, as shown in Fig. 5, the progressive change in $\bar{R}_\alpha$ and $\bar{R}_\gamma$ with time is notably far apart in $\alpha10$ system when compared to the rest. Nevertheless, this separation gets reduced with the increase in the volume fraction of minor phase α.

Analyses based on the coefficient of determination, in Fig. 4, unravel that the growth rate of duplex microstructure is predominantly influenced by evolution kinetics of major-phase grains. Moreover, the effect of the minor-phase grains decreases as their corresponding volume fraction reduces. Adopting these insights, and given that in Fig. 5 γ grains of $\alpha10$ exhibit maximum growth rate, it can be predicted that the overall growth kinetics of the corresponding microstructure will be noticeably greater than the other duplex systems considered in this study. Furthermore, it can also be stated that, since the volume fraction of minor phase continues to be considerably lower in $\alpha16$ and $\alpha33$, the overall growth will be dominated by the γ-phase grains, and their kinetics will correspondingly follow the $\alpha10$ microstructure. Finally, considering that the volume of phase α is close to the major phase in $\alpha40$, based on Fig. 4, it can be suggested that this duplex microstructure will represent the lower bound for the rate of evolution in the figure.

In order to verify the accuracy of the above predictions, emerging from the understanding of coefficient of determination, the overall growth rate exhibited by different duplex
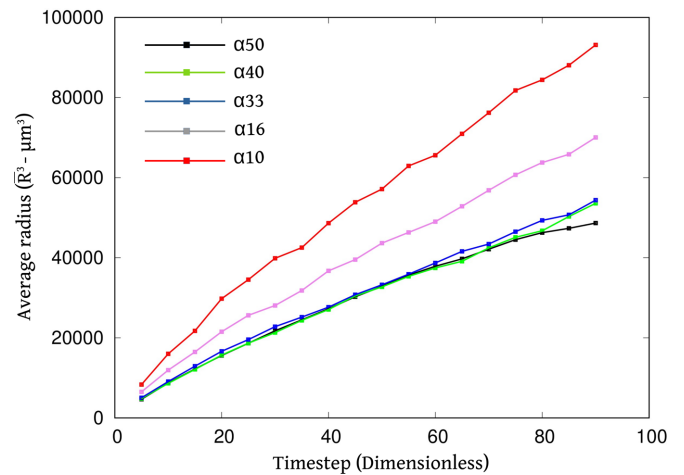
microstructures is cumulatively presented in Fig. 6. In complete adherence to the prediction, it is observed that, in duplex microstructures with unequal phase fraction, maximum and minimum growth rate, respectively, pertain to $\alpha10$ and $\alpha40$ microstructures. Additionally, the kinetics of evolution exhibited by $\alpha16$ and $\alpha33$ lies in-between the maximum and minimum, with the former noticeably greater than the latter. Ultimately, Fig. 6 affirms that, in duplex systems characterized by unequal volume fraction of constituent phases, the overall grain-growth kinetics is primarily governed by the evolution rate of the major-phase grains. This influence of the major-phase grains gets increasingly dominant with increase in its volume fraction.

5. Phase fraction and growth rate

Having realized that, for a given duplex microstructure, the overall grain-growth rate $(d\bar{R}/dt)$ is predominantly dictated by the kinetics adhered to by the major-phase grains $(d\bar{R}_\gamma/dt)$, attempts are made to relate the varying phase fractions to the observed growth rate across different systems. Kinetics rendered by the diffusion-governed mechanism in multiphase microstructure complies with the power law characterized by the exponent $n = 3$. Considering that the exponent remains unaltered, despite the varying phase fractions in multiphase systems, the disparity in the rate of grain growth can only be understood from the kinetic coefficient k, that relates the average radius to time. In other words, the effect of phase fraction on growth kinetics is efficiently described by relating the kinetic coefficient to the volume fraction of the major phase. To that end, evolution of duplex systems with different phase fractions is analyzed and the corresponding kinetic coefficient is ascertained. The resulting data set which includes volume fraction of the major phase (major-phase fraction), and the kinetic coefficient exhibited by the respective system, is handled through machine-learning techniques, particular regression analysis, in two different ways. First, an expression delineating the effect of major-phase fraction on the kinetic coefficient dictating the grain growth of duplex microstructure is ascertained. Subsequently, the resulting
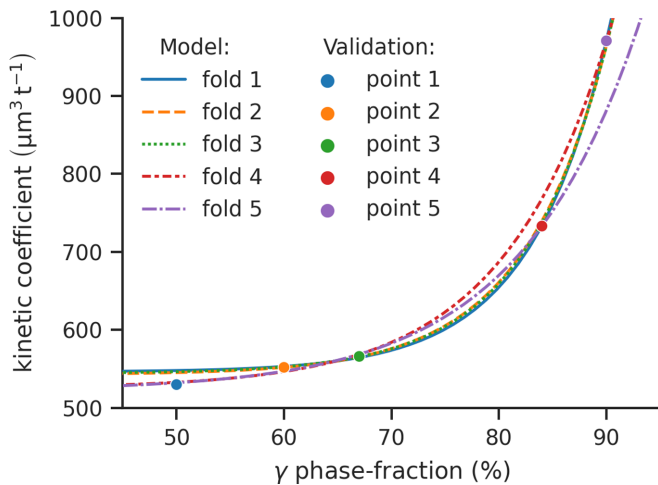
FIG. 7. Temporal change in the average radius of entire duplex systems $\bar{R}^3$ with varying phase fractions during grain growth.

predictive function is analyzed to critically assess its ability to handle unknown data, and to avoid overfitting.

A rather straightforward nonlinear regression treatment, wherein a hypersurface is introduced to fit the existing variables, is adopted to comprehend the data set encompassing major-phase fractions and kinetic coefficients of duplex microstructures (k_{dp}). As indicated in Fig. 7, the nonlinear regression treatment yields an exponential relation of the form

$$k_{dp} = A_{dp} + B_{dp} \exp(C_{dp} V_\gamma), \tag{11}$$

where V_γ is the volume fraction of the major phase γ, with A_{dp}, B_{dp}, and C_{dp} representing the adjustable model parameters. Moreover, in Eq. (11), k_{dp} is the kinetic coefficient which relates the temporal change in the average radius of the duplex microstructure with time, when expressed as a power law $R(t)^3 - \bar{R}_0 = k_{dp} t$. Despite the relation rendered by the conventional regression analysis, the underlying numerical treatment is extended and made more rigorous to enhance the predictive ability of Eq. (11) across the unknown information. This is achieved by appropriate tuning of the parameters A_{dp}, B_{dp}, and C_{dp} through extensive training of the underlying regression model.

Although the present numerical model renders thermodynamically consistent outcomes, the generated volume of information poses a crucial challenge. When compared to the wealth of information generally involved in machine-learning analyses, the data set describing the grain-growth kinetics of duplex microstructures with varying phase fractions is rather limited. Owing to the restricted size of the data set, an appropriate strategy, namely, "leave-one-out cross validation , is adopted to study the performance of the function in handling unknown data. By isolating one data point for testing, this validation approach develops a predictive model by training on the rest, and suitably initializing the parameters (A_{dup}, B_{dup}, and C_{dup}). This treatment is sufficiently iterated until all the data points separately assume the role of test data. The comparison of the different models, with characteristic parameters, emerging from the overlapping subsets of the original data, called "folds," yields an understanding on the susceptibility of overfitting and robustness of the predictions.

For the present cross-validation treatment, for each fold, the training utilizes a Levenberg-Marquardt solver. Moreover, a mean-squared error (MSE) loss function and a learning rate of 0.1 is adopted for 101 epochs of training that completely encompasses the data set of duplex microstructures.

The effect of the volume fraction of major phase (V_γ) on the kinetics coefficient dictating the grain growth in the duplex microstructure is illustrated in Fig. 7. Evidently, with increase in the major-phase fraction, the grain-growth kinetics of the two-phase system correspondingly increases. This influence of the major phase γ is captured by all models with characteristic *left-out* validation point. In Fig. 7, the left-out point for each fold, rendering its own predictive model, is indicated by using the same color of the line plot. This representation unravels that almost all models emerging from the respective folds exhibit substantial capability of handling unknown data. However, the largest deviation in prediction is observed while estimating the left-out point pertaining to fold 5. The performance of individual models on the training and test sets is quantitatively presented in Table IV, by ascertaining the corresponding mean absolute error (MAE). In keeping with Fig. 7, this tabulation reveals that, while the MAE of most predictive models is within the acceptable range, the corresponding value for fold 5 is considerably higher. This atypical deviation, exclusively emerging from fold 5, can be attributed to the steep gradients of exponential models towards the upper boundary, which correspondingly scales the generalization error. In other words, the unconvincing performance of the predictive model of fold 5 is primarily due to the exponential nature of the relation between the major-phase fraction and kinetic coefficient amplified by the position of the relevant data point. With increase in the information around the left-out point of fold 5, the predictability of the resulting mode can be significantly improved. Considering the computational cost to add to the existing data points, the perceived reason for the deviation and, more importantly, the performance of other models, the present discussion is confined to Fig. 7, which reflects the relation established in Eq. (11) between the volume fraction of the major phase and grain-growth kinetic coefficient of the duplex system.

B. Triplex microstructures

Triplex systems are characterized by the association of individual grains, in the polycrystalline setup, to one of the three constituent phases. The corresponding microstructure, in this study, comprises of phases α, β, and γ, with γ largely acting as the matrix or major phase. In the existing works, unlike duplex systems, very few three-phase microstructures with varying phase fractions are analyzed [32]. This limited consideration of triplex microstructure can largely be attributed to the computational burden associated with it. In the present study, on the other hand, grain growth in 14 different three-phase microstructures, with varying phase fractions, are examined to elucidate with statistical certainty how the evolution of the individual phase grains effects the growth kinetics of the entire triplex microstructure.

1. Grain-growth kinetics

Despite the difference in the number of phases, grain growth in both duplex and triplex systems is fundamentally

TABLE IV. Cross-validation performance for the duplex system, measured by the mean absolute error.

Fold	1	2	3	4	5
Training	0.01135	0.02881	0.02447	0.01507	0.03120
Validation	0.10656	0.04888	0.05206	0.19088	1.10930

governed by the same mechanism. Therefore, the grain growth in three-phase systems, which is dictated by the diffusion of chemical components, adheres to the power law with the exponent $n = 3$. In order to ensure that the grain growth in triplex systems is accurately modeled by the present approach, a preliminary validation strategy adopted for duplex microstructures is extended. Correspondingly, the temporally varying average radius of the individual phase grains $\bar{R}_\alpha$, $\bar{R}_\beta$, and $\bar{R}_\gamma$, and overall microstructure $\bar{R}$, is raised to different powers ($n = \{1, 2, 3, 4\}$) and related to time t. Correlation coefficients characterizing the different relations are ascertained for two triplex microstructures $\alpha33\beta33$ and $\alpha39\beta22$, and are graphically illustrated in Fig. 8.

It is evident in Fig. 8 that the correlation coefficient relating the average radius to the time is highest when $n = 3$ for both individual phases, and the overall microstructure. The maximum correlation exhibited by the cube of the different average radii $\bar{R}_\alpha$, $\bar{R}_\beta$, $\bar{R}_\gamma$, and $\bar{R}$ with time implies that the growth of the individual phase grains, and the entire microstructure, are predominantly governed by the long-range diffusion of the chemical components.

2. Ascertaining governing factor

Considering that grain growth in both duplex and triplex systems is predominantly dictated by the diffusion of the chemical components, phase fraction renders identical influence on the evolution of individual phases. In other words, when certain phase(s) assume minor volume fraction in the three-phase microstructure, owing to relative increase in the length, and complexity, of the diffusion path, the growth of the corresponding grains is stunted. On the other hand, the evolution kinetics is enhanced when the volume of the phase(s) is dominant in the multiphase systems. Apart from these generalized understandings, existing reports rarely offer

any further insights on the grain-growth kinetics in triplex microstructures. Particularly, similar to the duplex system, sufficient consideration has not been rendered to relate the growth kinetics of the individual phases to the evolution of the entire triplex system. To that end, in this analysis, the impact of the growth rate of individual phase grains on that entire three-phase microstructure is examined by ascertaining the corresponding coefficient of determination.

The instantaneous growth rate for constituent phase grains $d\bar{R}_\alpha/dt$, $d\bar{R}_\beta/dt$, and $d\bar{R}_\gamma/dt$, along with the entire triplex microstructure $d\bar{R}/dt$, is determined by monitoring temporal change in the respective parameter. These instantaneous growth kinetics of the individual phase grains are related to those of the entire microstructure, and the corresponding coefficient of determination is estimated through Eq. (8). For each system, three distinct coefficients of determination, χ_α, χ_β, and χ_γ, are estimated, reflecting the characteristic feature of the triplex microstructure. These coefficients of determinations are related to the phase fractions of the microstructure, and illustrated in Fig. 9.

In the triplex systems considered in this study, the volume fraction of phase γ reaches as low as 33% despite being the major phase. Such volume fraction of phase γ is noticed in the triplex microstructure characterized by equifraction of phases. Furthermore, in some systems like $\alpha45\beta10$, the phase α assumes a volume fraction of 45%, in spite of being one of the minor phases. This, and similar, understanding of phase
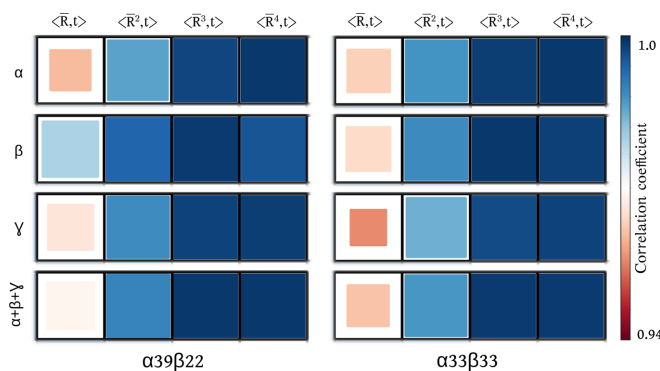

FIG. 8. Correlation coefficient characterizing the relation between time and average radius of individual phase grains and entire microstructure, raised to different powers ($n = 1, 2, 3$, and 4) for two triplex systems, $\alpha39\beta22$ and $\alpha33\beta33$.
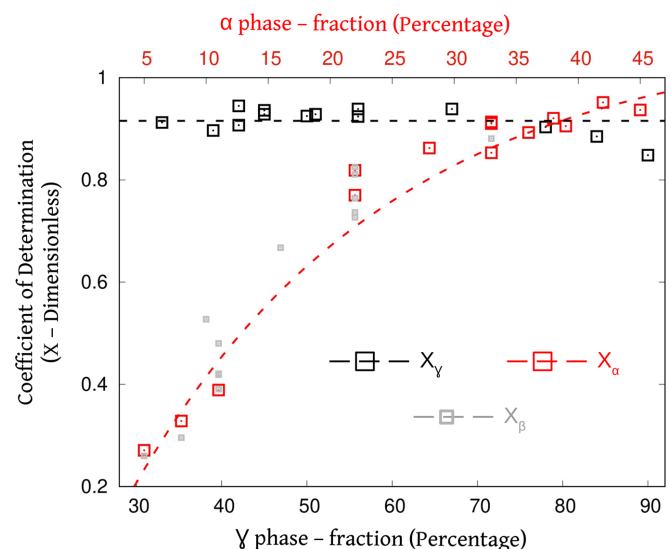

FIG. 9. Change in coefficient of determination, typifying the influence of growth rate of individual phase grains on the evolution kinetics of entire microstructure, with variation in the volume fraction of constituent phases.

fraction is vital to investigate the coefficients of determination presented in Fig. 9.

Figure 9 unravels that, even though the volume fraction of the major phase varies noticeably across different triplex systems, the corresponding coefficient of determination χ_γ continues to remain high. Given that phase γ stays as a major phase, despite the change in phase fractions, the high values of χ_γ can be attributed to the dominant volume of the respective grains. In other words, analogous to the duplex microstructure, the evolution kinetics of major-phase grains offers relatively greater influence on the overall growth rate exhibited by the entire triplex microstructure. Furthermore, Fig. 9 suggests that the coefficient of determination of the minor phases α and β noticeably increases as their corresponding volume fraction raises. Particularly, as the volume of phase α gets as dominant as γ, in a triplex system, an identical coefficient of determination is rendered, $\chi_\alpha = \chi_\gamma$. On the other hand, when the volume of the phases is minimal, the respective coefficient of determination assumes least value. Ultimately, it is evident from Fig. 9 that the influence of the individual phase grains on the overall growth kinetics depends largely on the corresponding volume fraction. In a triplex system with unequal volume fraction of phases, the growth rate of the entire microstructure $d\bar{R}/dt$ is predominantly governed by the evolution of the major-phase grains $d\bar{R}_\gamma/dt$. When the volumes of two phases are dominant in a three-phase system, the growth rate of both these phase grains offers identical influence on evolution of the microstructure. The contribution of particular phase grains to the overall evolution kinetics, $d\bar{R}/dt$, becomes least when its volume fraction is minimal. Based on the understanding rendered by Fig. 9, as demonstrated for duplex systems (Fig. 6), the growth kinetics of a triplex microstructure, in relation to others with varying phase fractions, can be predicted from the temporal change in the average radius of the corresponding phase-associated grains.

3. Interdependency in the evolving phases

In duplex systems, since the grains of the polycrystalline microstructure are associated with either of the two constituent phases, the evolution of a particular phase grain, and its kinetics, is inherently bound to each other. However, the same interdependency cannot be expected in triplex systems, wherein the grains can be associated with one of the three possible phases. Moreover, in three-phase microstructures, the level of influence offered by one evolving phase grain on the rest of the phase-associated grains has not been conscientiously addressed yet. Therefore, by examining the temporal change in the average radius of a particular phase grain in relation to the others, the interdependency exhibited between the phases, in triplex microstructures, during grain growth is elucidated.

Instead of investigating all the 14 triplex microstructures to explicate the effect of one evolving phase on the other, the systems are categorized based on phase fraction, and one microstructure from each category is analyzed. Since the coefficient of determination, which quantifies the effect of an evolving-phase grain on the growth of the overall triplex microstructure, depends on volume fraction, the phase-fraction-based grouping is deemed reasonable. Apart from
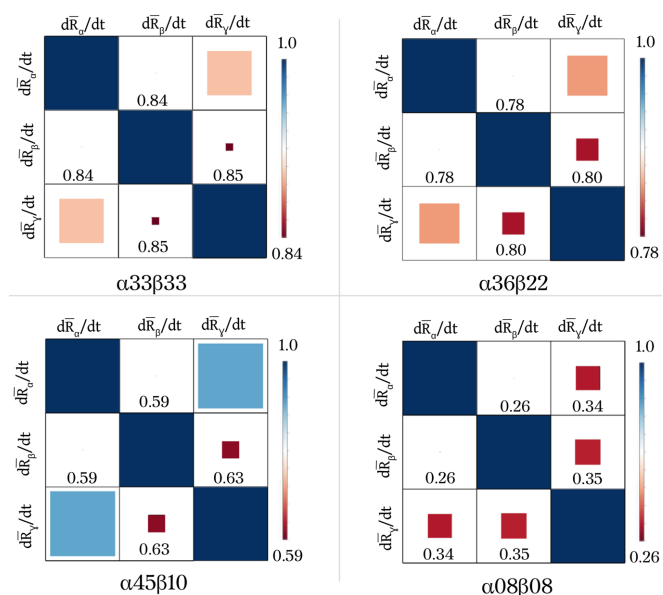

FIG. 10. Correlation coefficient explicating the interdependency between the growth rate of different phase grains $d\bar{R}_\alpha/dt$, $d\bar{R}_\beta/dt$, and $d\bar{R}_\gamma/dt$, during grain growth of four different triplex systems with varying phase fractions. (The values of correlation coefficients are included in certain sections to facilitate unambiguous interpretation of the illustrated relations.)

the equifraction system $\alpha33\beta33$, wherein all the constituent phases largely occupy similar volume, the remaining systems can be categorized as "equimajor," "equiminor," and "nonequifraction" triplex microstructures. While, in the equimajor system, the volume of one of the minor phases is equal to that of the major phase ($V_\alpha = V_\gamma$), the volume fraction of minor phases is identical in equiminor microstructures ($V_\alpha = V_\beta$). Moreover, the nonequifraction system stands in direct contrast to the equifraction microstructure, and is characterized by totally unequal volume fraction of the constituent phases ($V_\alpha \neq V_\beta \neq V_\gamma$).

In order to understand the degree of interdependency between the evolving phases, in addition to equifraction microstructure, grain growth exhibited systems $\alpha36\beta22$, $\alpha45\beta10$, and $\alpha08\beta08$ pertaining to nonequifraction, equimajor, and equiminor, respectively, are analyzed. Given that the primary focus of the present investigation is *not* to quantify the effect of an evolving-phase grain on the rest, but rather to qualitatively realize the degree of interaction between two phases, during grain growth in a triplex system, the coefficient of determination is not estimated. However, alternatively, the growth rate of different phase-associated grains is estimated, $d\bar{R}_\alpha/dt$, $d\bar{R}_\beta/dt$, and $d\bar{R}_\gamma/dt$, and is related to (or plotted against) each other. The correlation coefficient characterizing the relation between the growth rate of two phase grains is realized for predetermined triplex microstructures, and graphically illustrated in Fig. 10.

Before elucidating the level of interaction between two evolving phase grains in a given triplex microstructure, based on Fig. 10, it is exceedingly critical to realize the variation in the range of correlation coefficient across the different systems. Particularly, as opposed to the maximum value,

which remains constant at unity, the least value of the correlation coefficient changes with phase fraction. Correspondingly, Fig. 10 unravels that the lowest correlation coefficient in the equifraction system is maximum (0.84) when compared to the rest of the triplex microstructures, and it is respectively followed by nonequifraction ($\alpha36\beta22$) and equimajor ($\alpha45\beta10$) microstructures, with the absolute minimal exhibited by the equiminor system ($\alpha08\beta08$). This significant disparity in the lowest value of correlation coefficient emphasizes the importance of considering the context, i.e., the correlation-coefficient range, while interpreting the interaction between two phases in a given microstructure during grain growth. Apparently, the least interdependency between the two-phase grains in an equifraction system translates to a strong interaction in the context of equiminor triplex microstructure.

The graphical representation of correlation coefficient in Fig. 10 indicates the influence of the growth rate of a constituent phase grain on the evolution of the remnant grains during grain growth in triplex microstructures. Moreover, this depiction unravels similarities and dissimilarities across the triplex systems with varying phase fractions. It is evident in this illustration that, irrespective of the nature of the three-phase system, the correlation coefficient relating the growth rate of α- and β-phase grains is minimal, within a given microstructure. In other words, during grain growth in a triplex system, the evolution kinetics of a minor-phase grain imposes the least effect on growth rate of other low-volume phase grains. Despite being equifraction, largely owing the manner in which the triplex microstructure is initialized, such effect is also observed in $\alpha33\beta33$ microstructure. However, it is vital to note that the least correlation in equifraction system is tantamount to noticeable interaction in relation to other triplex microstructures. Therefore, in $\alpha33\beta33$ system, the evolution kinetics of one phase grain is generally interlinked with grains of the other phases, but this interaction is least between phases α and β.

Within a triplex system, during grain growth, Fig. 10 suggests that minimal interdependency following two minor phases is observed between the minor phase and the matrix grains, irrespective of the phase fractions. The only exception is the equiminor system wherein the volume fractions of the minor phases are identical. Furthermore, in all triplex systems, the growth rate of minor-phase grains with relatively greater volume fraction when compared to the other ($V_\alpha > V_\beta$) is strongly coupled with the evolution of the major-phase grains. Ultimately, the study of interdependency between the rate of the evolving phase grains during grain growth in triplex systems, using correlation coefficients, unravels that a general trend is observed in three-phase microstructures irrespective of the phase fractions. If we distinguish the constituent phases as minor, inter, and major phases depending on their corresponding volume fractions, which in the present study are α, β, and γ, respectively, then the least interaction during grain growth is exhibited by the minor-phase and interphase grains. While the growth rate of major-phase grains is considerably interlocked with the interphase grains, the effect of the minor phase on the matrix is comparatively lower. In other words, in a given triplex microstructure, the level of influence offered by the evolution rate of one phase grain on the other, during grain growth, is primarily dictated by their corresponding vol-

ume fractions. When the volume fractions of two phases are minimal, their degree of interaction is also minimal, whereas a considerable dependency is noticed when the volumes of the two phases are dominant in view of the third.

The above analysis on the interdependency of the kinetics of evolving phases in triplex system unravels that, for expressing the overall growth rate of a three-phase microstructure, the two ideal variables are the evolution rate of the grains of minor phases, prescribed by the least *multicollinearity*.

4. Phase fraction and growth rate

A principal insight rendered by this study is that, in grain growth, the evolution rate of a multiphase system is primarily governed by the volume fraction of its constituent phases through their respective growth kinetics. Therefore, by relating the phase fraction of 14 different triplex microstructures, considered in this work, to its corresponding growth kinetics, an attempt to extract a generalized expression is made. Unlike the duplex system, since triplex microstructures are characterized by three constituent phases, the corresponding evolution rate is dictated by two independent variables, i.e., volume fractions. By directly relating the volume fraction, instead of the evolution rate of individual phase grains, to the growth kinetics exhibited by the triplex systems, the question of multicollinearity is obviated.

Similar to the analysis of two-phase systems, nonlinear regression can be extended to the multivariate framework for relating the phase fractions of triplex system to the corresponding grain-growth kinetics. Such treatment would yield an expression of the form $k_{\mathrm{tr}} = A_{\mathrm{tr}} + B_{\mathrm{tr}} \exp(C_{\mathrm{tr}}^\alpha V_\alpha + C_{\mathrm{tr}}^\gamma V_\gamma)$, with k_{tr} representing the growth kinetics of triplex system and model parameters denoted by A_{tr}, B_{tr}, C_{tr}^α, and C_{tr}^γ. Despite capturing the general trend in the effect of volume fractions V_α and V_γ, on the evolution rate, the above relation is not rigorous enough to adequately account for the local variations. To that end, generic models with adjustable variance and biases, that are capable of encompassing local characteristic relations surrounding the data points, through several tunable parameters, are developed to realize the influence of phase fractions on grain growth exhibited by three-phase systems. Predictive models are generated by adopting a simple dense feed-forward neural network technique which can be expressed as

$$\boldsymbol{a}^{(l)} = \mathrm{f}\big(\boldsymbol{W}^{(l)}\boldsymbol{x}^{(l)} + \boldsymbol{b}^{(l)}\big) \quad \text{for all } l = 1, \ldots, L \qquad (12)$$

with $\boldsymbol{x}^{(0)} = [V_\alpha, V_\gamma)]^\mathsf{T}, \quad \boldsymbol{a}^{(l)} = \boldsymbol{x}^{(l-1)}, \quad \boldsymbol{a}^{(L)} = k_{\mathrm{tr}}, \quad (13)$

where $\boldsymbol{W}^{(l)}$, $\boldsymbol{b}^{(l)}$, and L indicate the weights, biases, and number of layers, respectively. In Eq. (12), the input and output to the layers are respectively denoted by $\boldsymbol{x}^{(l)}$ and $\boldsymbol{a}^{(l)}$, with $f(\cdot)$ indicating nonlinear activation function. While these hyperparameters are tuned by the users, the model parameters handled as a tensor get adjusted and reflect the data.

In the context of leave-one-out cross validation, the generality of the predictive models is ensured by preventing the information leak from the validation data into the hyperparameters. In other words, for each fold, though the model parameters are independently initialized and evaluated, the optimal hyperparameters remain unaltered. These

TABLE V. Cross-validation performance for the triplex system, measured by the mean absolute error.

Fold	1	2	3	4	5	6	7	8	9	10	11
Training	0.212	0.243	0.278	0.224	0.250	0.319	0.244	0.204	0.196	0.163	0.230
Validation	0.157	0.086	0.150	0.025	0.018	0.191	0.232	0.290	0.767	0.774	4.406

hyperparameters are tuned through a single fold using hyperband algorithm [58] and, subsequently, the best values are ascertained through the mean absolute error computed on a validation set through the approach involving a single hidden layer of 208 rectifier neurons and a learning rate of 0.03. Adam optimizer is employed for foldwise training of 101 epochs with a constant batch size of 4 [59]. The corresponding learning rate is tuned with the same algorithm as the architecture hyperparameters. In order to regularize the model, "early stopping" is used, which terminates the optimization when the performance is not improved for five consecutive epochs on the validation set.

The data points indicating the phase fractions of the different triplex microstructures, and predictions offered by the independently trained generic model for each fold, are collectively illustrated in Fig. 11. The distribution of the data points reflects the sample set of volume fractions considered for the current investigation, as depicted in Fig. 1. However, it is evident from Fig. 11 that the kinetic coefficients are sensitive to the local scattering of the points and correspondingly vary. The ability to capture these variations in the kinetic coefficients vindicates the use of generic models as opposed to the nonlinear regression technique. In other words, generic models, particularly dense neural networks used in this study, ensure that domains of interest with strong local differences are accurately mapped though adjustable parameters. In Fig. 11, though the independently trained models yield different mappings, the similarity characterized by plateau (left side, $0\% < V_\gamma < 60\%$) and gradient regions (bottom right, $75\% < V_\gamma < 100\%$) is noticeable. Moreover, the morphology of the plateau, in all folds, changes across the training (known) and validation (unknown) data points. The gradient regions complementing the shapes of the plateaus remain comparable with the contours.

Table V summarizes the mean absolute error (MAE) performances of each model of the cross validation. Compared with the exponential model for the duplex case, validation and training performance are closer, which can be attributed to a suitable regularization combined with sufficient capacity of the low-bias neural-network model, allowing a robust performance even on tiny data sets with strong nonlinear characteristics. Towards high values of V_γ, these kinds of generic models are subjected to the same data-set-inherent problems as the exponential model, i.e., the steep gradients of the physical behavior demand a considerably higher number of data points to reduce the error.

The nonlinear regression treatment extended to triplex systems. as illustrated in Fig. 11, unravels that the kinetic coefficient, principally dictating the rate of grain growth, can be definitively related to the independent volume fractions of the constituent phases in the three-phase microstructures. In other words, in spite of the limitations imposed by the size of the data set, the extended regression analyses sug-

gest an exponential trend, similar to two-phase systems, between the phase fractions and the corresponding grain-growth kinetics in triplex microstructures. Correspondingly, it is indicative that the rate of grain growth in multiphase systems, with a given combination of phases, can be significantly varied by exclusively altering their respective volume fractions. The relation between the phase fraction and kinetic coefficient, realized for duplex and triplex systems in Figs. 7 and 11, is of an elegant form which could directly be extended to other multiphase systems and, more importantly, adopted for suitably regulating the rate of grain growth.

IV. CONCLUSION

Grain growth in polycrystalline systems can be desirable in some circumstances while undesirable in others. For instance, grain growth is induced during a processing technique to establish required average grain size, while noticeable measures are generally taken to avoid it during a given application. The subjective role of grain growth extends beyond homogeneous polycrystalline system to multiphase microstructures as well. Therefore, it becomes vital to understand the grain-growth kinetics exhibited by highly applicable multiphase polycrystalline microstructures associated with duplex and triplex systems. Particularly, generalized insights that aide in comprehending the growth rate of multiphase microstructures with varying phase fraction are exceedingly critical, as they can be adopted for a wide range of systems and application. To that end, in this study, the grain-growth kinetics of duplex and triplex systems is studied by employing approachable statistical techniques.

Conventionally, the grain-growth kinetics associated with multiphase systems is discussed by considering the evolution rate of individual phase grains and the entire microstructure separately. Such treatments rarely offer much insights on how the growth kinetics of individual phases relates to the overall evolution rate exhibited by the entire system. Therefore, in this work, sufficiently equipped statistical tools are employed to realize the effect of the constituent phases, and their corresponding grains, on the grain-growth kinetics of the multiphase microstructure.

The understanding gained from the current investigation on a wide range of microstructures encompassing two and three phases can succinctly be delineated in the following manner:

(1) The evolution rate of a complete multiphase microstructure is predominantly governed by the growth rate of major-phase grains, wherein the major and minor phases are distinguished exclusively based on volume fraction. This effect of major phase is particularly interesting considering that the evolution kinetics of the minor-phase grains is noticeably lower. Aside from statistical analyses, conventional treatment and corresponding elucidation affirm the dominant
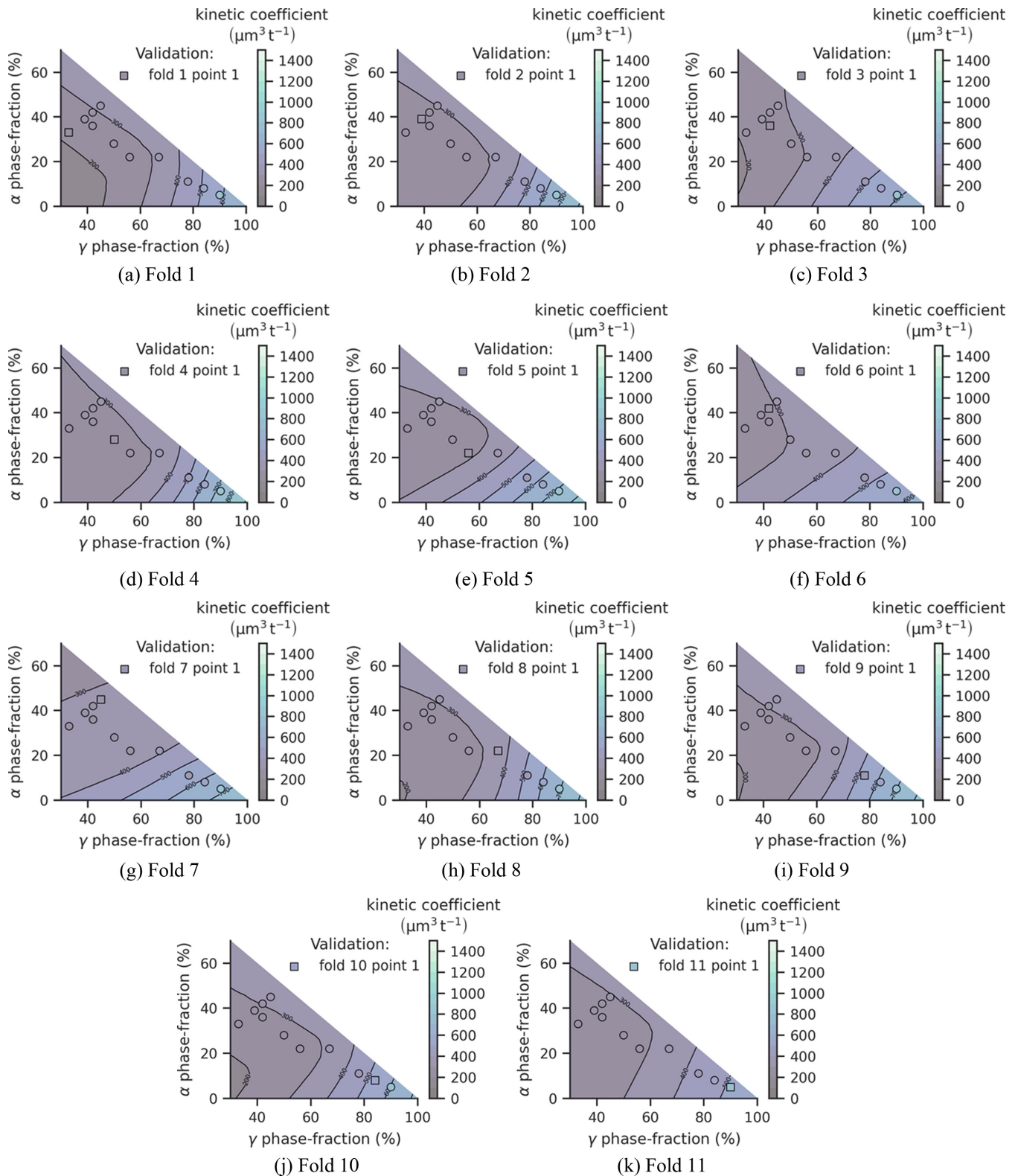
FIG. 11. Effect of phase fraction on the kinetic coefficient governing the rate of grain growth in triplex systems.

role of major-phase grains on the grain growth of the duplex and triplex microstructures. At the outset, the dominant influence of the major-phase grains on the temporal change in the average grain size of the multiphase polycrystalline microstructures *might appear obvious*. However, this study goes well beyond the apparent static relation between average radii of the major-phase grains and overall microstructure, and *essentially unravels the governing influence of the kinetics of major-phase grains on the grain-growth rate of the multiphase systems.*

(2) The relative effect of different phases on the overall curvature-driven transformation is realized by models that predict the kinetic coefficient of a given system from the characteristic phase fractions. These predictive models, validated by appropriate technique, indicate that a nonlinear exponential relation exists between the phase fractions and the kinetic coefficient in both duplex and triplex microstructures.

Aside from statistical comprehension of a principal phase dictating the overall grain-growth kinetics, the development of predictive models enhances the applicability of the present analysis. Owing to its thermomechanical properties, alumina is used in high-temperature applications. However, grain growth induced in polycrystalline alumina compromises its function be altering the relevant properties. Consequently, chromia (Cr_2O_3) is included in polycrystalline alumina to inhibit grain growth. The amount of chromia in alumina, i.e., phase fraction, is generally varied in experimental studies to understand its effect on the kinetics [60]. Even though this approach yields a quantitative result, it can be made significantly efficient by employing the predictive model developed in this work. The model would essentially aide in narrowing down a specific range of phase fractions that adequately suppress grain growth without compromising other thermomechanical properties. The predictive model, developed for triplex systems, can analogously be adopted to identify a definite phase fraction in three-phase zirconium diboride ceramic of silicon and zirconium carbide, that ensures microstructural stability during its high-temperature application [23].

In systems wherein the phase fractions cannot be sufficiently varied, owing to its undesired effect on properties, the present analysis offers an alternate means for stunting the curvature-based microstructural evolution. Correspondingly, aside from altering the phase fraction, desired effective conductivity in solid-oxide fuel cells (SOFC), with triplex electrode, can be sustained by lowering the growth kinetics of the major-phase grains [24]. Furthermore, the predictive models and associated insights offered in this work can aide in perfecting sintering cycle, involved in the fabrication of multiphase nanocomposites, wherein introduction grain growth is ill preferred [53,61].

Even though the understanding rendered by the present investigation can be exploited for various purposes, one critical utilization would be to alter the grain-growth rate of a given multiphase system, with a definite phase fraction, by appropriately, and exclusively, varying the evolution kinetics of the major-phase grains. To that end, in the upcoming works, attempts will be made to substantiate the approach of modifying the grain-growth rate in multiphase systems by employing the dominant influence of the major-phase grains. Additionally, owing to the strong inclination of the current analyses to unravel the effect of phase fractions on the overall grain-growth kinetics in multiphase microstructures, identical and rather straightforward material parameters, including diffusivities, equilibrium concentrations, and interfacial energies, have been assigned to the various systems. Despite

deviating from the physical conditions, such considerations facilitate in isolating the influence of phase fraction. However, given the importance of the material parameters in dictating grain-growth evolution and its kinetics, the present approach would be quantitatively enhanced in the subsequent studies.

APPENDIX A: EXPANDING GOVERNING EQUATIONS

In the current investigation, grain growth in several multiphase systems is principally modeled by taking the variational derivative of the functional expressed in Eq. (5). This derivative dictating the spatiotemporal evolution of the phase field, in Eq. (6), translates to the transformation of the polycrystalline microstructures. The energy contribution of the diffuse interfaces in the overall functional $\mathcal{F}(\boldsymbol{\phi}, \nabla\boldsymbol{\phi}, \boldsymbol{c})$ reads as

$$f_{\text{int}}(\boldsymbol{\phi}, \nabla\boldsymbol{\phi}) = \varepsilon a(\boldsymbol{\phi}, \nabla\boldsymbol{\phi}) + \frac{1}{\varepsilon} w(\boldsymbol{\phi}), \qquad (A1)$$

wherein $\varepsilon a(\boldsymbol{\phi}, \nabla\boldsymbol{\phi})$ and $\frac{1}{\varepsilon} w(\boldsymbol{\phi})$, respectively, indicate the gradient-energy density and obstacle potential [62]. Summation of all possible pairwise interaction between chemically similar and dissimilar grains yields the gradient-energy density, which is correspondingly formulated as

$$\varepsilon a(\boldsymbol{\phi}, \nabla\boldsymbol{\phi}) = \sum_{\alpha \leqslant \beta}^{N} \sum_{m \leqslant n}^{q_\alpha} \gamma_{\alpha\beta}^{mn} \left| \boldsymbol{\mathcal{Q}}_{\alpha\beta}^{mn} \right|^2. \qquad (A2)$$

In Eq. (A2), the energy of the grain boundary separating grains m and n of α and β phases is represented by $\gamma_{\alpha\beta}^{mn}$. Furthermore, $|\boldsymbol{\mathcal{Q}}_{\alpha\beta}^{mn}|^2$ which adds to the interface-energy contribution is the gradient vector and is written as

$$\boldsymbol{\mathcal{Q}}_{\alpha\beta}^{mn} = \phi_\alpha^m \nabla\phi_\beta^n - \phi_\beta^n \nabla\phi_\alpha^m. \qquad (A3)$$

Although a suitable formulation of the Eq. (A2) would facilitate the introduction of anisotropy, in the present investigation, identical energies are attributed to all the different grain boundaries of the multiphase systems. Aside from gradient-energy density in Eq. (A2), the contribution of the diffuse interface to the principal energy functional includes $\frac{1}{\varepsilon} w(\boldsymbol{\phi})$, the potential-energy density. This obstacle-type penalizing potential which ensures that the phase fields, at any given spatial position, add up to unity, in the present model, is devised through the Gibbs simplex of the form

$$\mathcal{G} = \left\{ \boldsymbol{\phi} \in \mathbb{R}^{\bar{N}} : \sum_{\alpha}^{N} \sum_{m}^{q_\alpha} \phi_\alpha^m = 1, \phi_\alpha^m \geqslant 0 \right\}. \qquad (A4)$$

Based on the simplex $\mathcal{G}$, the penalizing potential-energy density is correspondingly expressed as

$$\frac{1}{\varepsilon}\omega(\boldsymbol{\phi}) = \begin{cases} \frac{1}{\varepsilon}\left(\frac{16}{\pi^2} \sum\limits_{\alpha \leqslant \beta} \sum\limits_{m \leqslant n} \gamma_{\alpha\beta}^{mn} \phi_\alpha^m \phi_\beta^n + \sum\limits_{\alpha \leqslant \beta \leqslant \delta} \sum\limits_{m \leqslant n \leqslant p} \gamma_{\alpha\beta\delta}^{mnp} \phi_\alpha^m \phi_\beta^n \phi_\delta^p \right), & \boldsymbol{\phi} \in \mathcal{G} \\ \infty, & \boldsymbol{\phi} \notin \mathcal{G} \end{cases} \qquad (A5)$$

while the obstacle potential for all grain boundaries is introduced through the first term, the higher-order second term prevents the introduction of any spurious phases, by imposing an energy constraint.

Equilibrium concentration characterizing specific phases is assigned to grains to establish multiphase systems with definite and stable phase fraction. Despite the chemical equilibrium, the curvature difference introduced by the dissimilarities in the sizes and morphology of the grains induces a mass transfer that facilitates the growth of larger grains, of a given phase, at the expense of the smaller ones. This migration of solute i, principally driven by the curvature (K), can be written as

$$\frac{\partial c_i(\mu_i(K), \phi)}{\partial t} = \left(\frac{\partial c_i}{\partial \mu_i(K)}\right)_{\phi_\alpha^m} \frac{\partial \mu_i(K)}{\partial t} + \left(\frac{\partial c_i}{\partial \phi_\alpha}\right)_{\mu_i} \frac{\partial \phi_\alpha^m}{\partial t}.$$
(A6)

Rearranging the above formulation yields the evolution of chemical (diffusion) potential as expressed in Eq. (7). Considering that the evolution of the chemical (diffusion) potential is formulated based on the temporal change in the concentration, both these principal variables are "implicitly" coupled. (For complete derivation, the readers are directed to Ref. [42].) Owing to the computational efficiency, and characteristic of the current grand-potential approach, the chemical (diffusion) potential is treated as the fundamental variable instead of the concentration.

Even though as opposed to concentration, the evolution of the chemical (diffusion) potential dictates grain growth in the present formulation, the kinetics of the evolution is influenced by the mobility $M(\phi)$, as indicated in Eq. (7). The mobility which includes interdiffusivity and susceptibility matrix reads as

$$M(\phi) = \sum_{\alpha=1}^{N} D_{\alpha:i}\left(\frac{\partial c_i^\alpha}{\partial \mu_j}\right)\sum_{m}^{q} h(\phi_\alpha^m) + \sum_{\alpha}^{N} D_{\alpha\alpha:i}\sum_{m<n}^{q,q}\left[\left(\frac{\partial c_i^\alpha}{\partial \mu_j}\right)h(\phi_\alpha^m) + \left(\frac{\partial c_i^\beta}{\partial \mu_j}\right)h(\phi_\alpha^n)\right]\phi_\alpha^m \phi_\alpha^n$$

$$+ \sum_{\alpha}^{N}\sum_{\alpha<\beta}^{N} D_{\alpha\beta:i}\sum_{m\leqslant n}^{q,q}\left[\left(\frac{\partial c_i^\alpha}{\partial \mu_j}\right)h(\phi_\alpha^m) + \left(\frac{\partial c_i^\beta}{\partial \mu_j}\right)h(\phi_\beta^n)\right]\phi_\alpha^m \phi_\beta^n.$$
(A7)

In the above formulation, while the bulk diffusivity is indicated by $D_{\alpha:i}$, the kinetics of the solute migration along interfaces of the similar and dissimilar grains is effected by matrices $D_{\alpha\alpha:i}$ and $D_{\alpha\beta:i}$, respectively. These matrices are symmetric and of size N × N [42]. Moreover, in Eq. (A7), $\frac{\partial c_i^\alpha}{\partial \mu_j}$ represents the susceptibility matrix.

APPENDIX B: REALIZING OVERFITTING

When the variables including average radius and time are related by *power law* [$f(x) = ax^n$], the correlation coefficient *generally* increases with raising the order of the expression n. In other words, the correlation between x and $f(x)$ will often be higher when $n = m$, as opposed to $n = m - 1$, where $m \in \mathcal{N}$. In such instances, which is most, identifying the best relation based on the correlation coefficient alone is rather ineffective, as the next order $n + 1$ would offer a more convincing fit. Therefore, with increase in the order, the corresponding change in the correlation coefficient is estimated. For a given raise in the order, when the change in the correlation coefficient is marginal, then the resulting relation is deemed overfitting. Although for a given data set, an overfitted expression convincingly relates all the existing data points, it rather fails significantly when new data are augmented. Stated otherwise, an overfitted hyperplane is restricted to a specific set of data points; any variation to the data would render the existing fit noticeably inaccurate. Consequently, the order that precedes the overfitting is considered to be the best fit. Based on this statistical understanding, certain orders in Figs. 3 and 8 are treated as overfitting, while a lower n is deemed as best fit.

In contradiction to the generally expected continual increase, when there is a decrease in correlation coefficient with

the order, the consideration of the overfitting is relaxed. Moreover, in such instances, the order with maximum correlation coefficient is deemed to reflect the best fit. Such decrease in the correlation coefficients with increase in n is noticeable in Figs. 3 and 8, wherein the corresponding best fit is realized from the highest correlation coefficient.

APPENDIX C: INTERDEPENDENCY IN DUPLEX SYSTEMS

In a polycrystalline system, irrespective of its nature, the continuum is established by the multiple grains present it. During the grain growth, despite the continual disappearance of the grains, the continuum is sustained by the growth the surviving grains. This characteristic feature of the grain growth introduces interdependency between the evolving grains. Correspondingly, in duplex systems, wherein the grains are associated with one of the two-constituent phases, the evolution of phase-α grains is inherently linked the grains of phase γ. Even though the interaction between the phase-associated grains, during grain growth of a duplex system, can be theoretically conceived, to explicate it with a statistical certainty, the average radius of α grains, at a given time t, is plotted against the corresponding radius of γ grains in Fig. 12 for a two-phase microstructure with equal volume fraction of phases, $\alpha 50$. The trend in this illustration indicates an inherent interlocking between the evolution of the phase-α and -γ grains during the grain growth of equifraction duplex microstructure. In addition to the $\alpha 50$ microstructure, the average radius of constituent phase grains, at a given instance, is ascertained for a duplex system with 10% minor phase α. Similar to the equifraction system, these instantaneous average radii of phase α and γ grains are plotted against
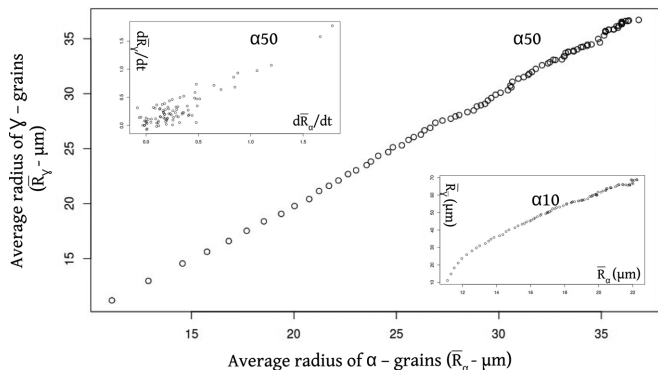
FIG. 12. The average radius of phase-α grains, at a given instance, is plotted against the corresponding radius of matrix-phase grains for duplex microstructure with equal volume fraction of phases. In the subplots, for the same system, the growth rate of individual phase grains is related, and instantaneous average radius of phase α and γ grains is plotted for duplex microstructure with 10% alpha.

each other, and illustrated in Fig. 12 as a subplot. Despite the change in the phase fraction, in $\alpha10$ microstructure as well, a definite interaction between the radius of major- and minor-phase grains is evident.

Aside from the average radius of the phases α and γ at a given instance, using the same approach, the relation between the kinetics of grain growth associated with these phases can be explicated. Correspondingly, the evolution kinetics of the α grains is related to that of the γ ones, for equifraction duplex microstructure, and are included as a subplot in Fig. 12. This illustration unravels that even though there exists a perceivable interdependency between the instantaneous kinetics of phase-α and -γ grains, it is not as straightforward as the average radius.

APPENDIX D: EFFECT OF INDIVIDUAL PHASE-GRAIN KINETICS ON GROWTH RATE OF ENTIRE SYSTEM

One of the primary aims of the present investigation is to realize the effect of individual phases on grain-growth rate of an entire two-phase microstructure. Particularly, the role of evolution kinetics of a given phase grain on the overall growth rate of a duplex system. To that end, the kinetics of evolution exhibited by phase-α grains, at a given instance, is related to the overall growth rate of equifraction duplex system, and plotted in Fig. 13(a). The graphical illustration relating the evolution rate of phase-α grains and duplex microstructure with 10% minor phase is included as a subplot.

Figure 13(a) unravels that the growth rate of phase-α grains imposes a definite influence on the overall kinetics exhibited by the equifraction-duplex system, $\alpha50$, during grain growth. On the other hand, the subplot of the corresponding illustration, which pertains to two-phase microstructure with 10% of phase α, indicates a relation between $d\bar{R}_\alpha/dt$ and $d\bar{R}/dt$ is not as definite as one noticed in the equifraction microstructure. It is the degree of inter-relation between the kinetics of individual phase grains, and overall growth rate of a given duplex microstructure, which varies with the phase fraction, is realized by *coefficient of determination*. In other words, while the coefficient of determination relating the $d\bar{R}_\alpha/dt$ and $d\bar{R}/dt$ will be higher for an equifraction duplex microstructure, in $\alpha10$ system it will assume a relatively low value reflecting a not so definite relation between the kinetics.

In Fig. 13(b) the grain-growth kinetics of phase-γ grains and entire duplex system, with equal volume fraction of phases, is plotted against each other. As a subplot, the corresponding relation between $d\bar{R}_\gamma/dt$ and $d\bar{R}/dt$ for $\alpha10$ duplex microstructure with 10% of phase α is illustrated. Unlike the influence of phase α on overall growth kinetics in Fig. 13(a), a highly definite relation is observed between the evolution rate of phase-γ grains and entire microstructure in both equifraction and $\alpha10$ duplex microstructure. Consequently, the corresponding values of coefficient of determination will largely be independent of the phase fraction.
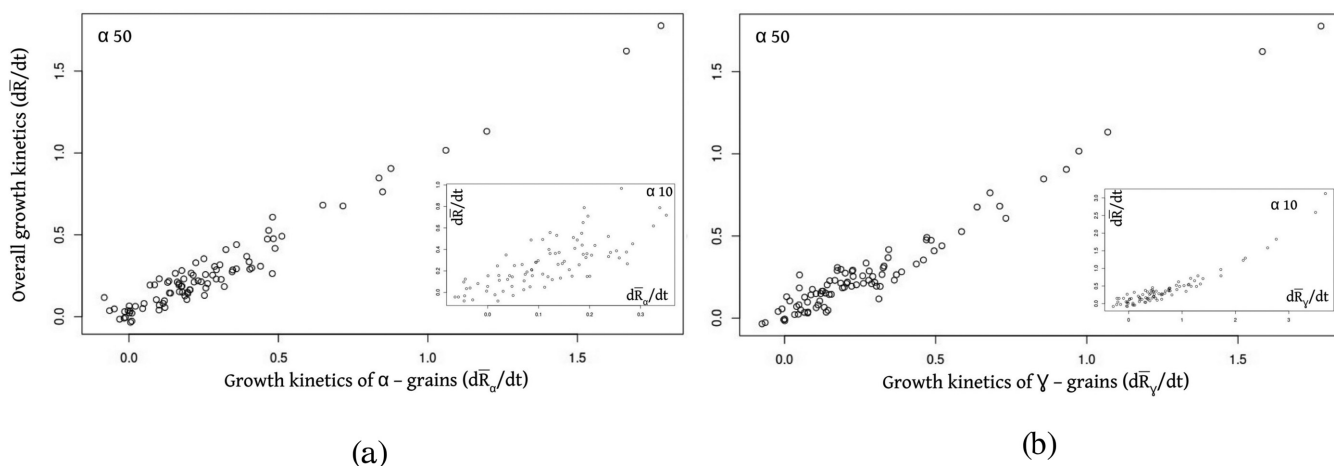

(a)

(b)

FIG. 13. The instances of grain-growth rate exhibited by an individual phase grain are plotted with respect to that of the entire duplex microstructure with equal volume fraction of phases. In (a) the kinetics of α grains is related to the grain-growth rate of the entire microstructure, while γ-grains evolution kinetics is considered (b). The corresponding outcomes for $\alpha10$ microstructure with 10% of minor phase α are included as subplots.

[1] P. Jacques, E. Girault, P. Harlet, and F. Delannay, The developments of cold-rolled trip-assisted multiphase steels. Low silicon trip-assisted multiphase steels, ISIJ Int. **41**, 1061 (2001).

[2] Y. Huang, C. Zhao, X. Lv, H. Wang, and J. Wu, Multiphase coexistence and enhanced electrical properties in $(1-x-y)BaTiO_3-xCaTiO_3-yBaZrO_3$ lead-free ceramics, Ceram. Int. **43**, 13516 (2017).

[3] A. Kumar, K. Sharma, and A. R. Dixit, Carbon nanotube- and graphene-reinforced multiphase polymeric composites: review on their properties and applications, J. Mater. Sci. **55**, 2682 (2020).

[4] X. Zhang, A. Godfrey, X. Huang, N. Hansen, and Q. Liu, Microstructure and strengthening mechanisms in cold-drawn pearlitic steel wire, Acta Mater. **59**, 3422 (2011).

[5] J.-K. Hwang, The microstructure dependence of drawability in ferritic, pearlitic, and twip steels during wire drawing, J. Mater. Sci. **54**, 8743 (2019).

[6] M. Liljas, P. Johansson, H.-P. Liu, and C.-O. A. Olsson, Development of a lean duplex stainless steel, Steel Res. Int. **79**, 466 (2008).

[7] A. Armas, C. Petersen, R. Schmitt, M. Avalos, and I. Alvarez-Armas, Mechanical and microstructural behaviour of isothermally and thermally fatigued ferritic/martensitic steels, J. Nucl. Mater. **307**, 509 (2002).

[8] R. Filip, K. Kubiak, W. Ziaja, and J. Sieniawski, The effect of microstructure on the mechanical properties of two-phase titanium alloys, J. Mater. Process. Technol. **133**, 84 (2003).

[9] S. Gollapudi, R. Sarkar, U. C. Babu, R. Sankarasubramanian, T. Nandy, and A. Gogia, Microstructure and mechanical properties of a copper containing three phase titanium alloy, Mater. Sci. Eng., A **528**, 6794 (2011).

[10] Z. Tang, O. N. Senkov, C. M. Parish, C. Zhang, F. Zhang, L. J. Santodonato, G. Wang, G. Zhao, F. Yang, and P. K. Liaw, Tensile ductility of an AlCoCrFeNi multi-phase high-entropy alloy through hot isostatic pressing (HIP) and homogenization, Mater. Sci. Eng., A **647**, 229 (2015).

[11] K. Liu, M. Komarasamy, B. Gwalani, S. Shukla, and R. S. Mishra, Fatigue behavior of ultrafine grained triplex $Al_{0.3}CoCrFeNi$ high entropy alloy, Scr. Mater. **158**, 116 (2019).

[12] B.-K. Jang, M. Enoki, T. Kishi, and H.-K. Oh, Effect of second phase on mechanical properties and toughening of Al_2O_3 based ceramic composites, Compos. B. Eng. **5**, 1275 (1995).

[13] E. H. Lutz, N. Claussen, and M. V. Swain, K^R-curve behavior of duplex ceramics, J. Am. Ceram. Soc. **74**, 11 (1991).

[14] E. W. Neuman, G. E. Hilmas, and W. G. Fahrenholtz, A high strength alumina-silicon carbide-boron carbide triplex ceramic, Ceram. Int. **43**, 7958 (2017).

[15] L. Feng, W. G. Fahrenholtz, and G. E. Hilmas, Effect of ZrB_2 content on the densification, microstructure, and mechanical properties of ZrC-SiC ceramics, J. Eur. Ceram. Soc. **40**, 220 (2020).

[16] A. Do Nascimento, V. Ocelík, M. Ierardi, and J. T. M. De Hosson, Microstructure of reaction zone in WCp/duplex stainless steels matrix composites processing by laser melt injection, Surf. Coat. Technol. **202**, 2113 (2008).

[17] M. Sternitzke, Structural ceramic nanocomposites, J. Eur. Ceram. Soc. **17**, 1061 (1997).

[18] D. Fan and L.-Q. Chen, Computer simulation of grain growth and Ostwald ripening in alumina–zirconia two-phase composites, J. Am. Ceram. Soc. **80**, 1773 (1997).

[19] Y. Yu, F. Lin, Y. Zheng, W. Yu, X. Liu, Y. Yuan, H. Yin, and X. He, High-density nanoprecipitation mechanism and microstructure evolution of high-performance Al_2O_3/ZrO_2 nanocomposite ceramics, J. Eur. Ceram. Soc. **41**, 5269 (2021).

[20] J. Cahn, Stability, microstructural evolution, grain growth, and coarsening in a two-dimensional two-phase microstructure, Acta Metall. Mater. **39**, 2189 (1991).

[21] D. Fan and L.-Q. Chen, Diffusion-controlled grain growth in two-phase solids, Acta Mater. **45**, 3297 (1997).

[22] W.-M. Guo, G.-J. Zhang, and P.-L. Wang, Microstructural evolution and grain growth kinetics in ZrB_2–SiC composites during heat treatment, J. Am. Ceram. Soc. **92**, 2780 (2009).

[23] H.-L. Liu, G.-J. Zhang, J.-X. Liu, and H. Wu, Synergetic roles of ZrC and SiC in ternary ZrB_2–SiC–ZrC ceramics, J. Eur. Ceram. Soc. **35**, 4389 (2015).

[24] Y. Lei, T.-L. Cheng, and Y.-H. Wen, Phase field modeling of microstructure evolution and concomitant effective conductivity change in solid oxide fuel cell electrodes, J. Power Sources **345**, 275 (2017).

[25] Y. Saito and M. Enomoto, Monte Carlo simulation of grain growth, ISIJ Int. **32**, 267 (1992).

[26] K. Kawasaki, T. Nagai, and K. Nakashima, Vertex models for two-dimensional grain growth, Philos. Mag. B **60**, 399 (1989).

[27] M. Anderson, D. Srolovitz, G. Grest, and P. Sahni, Computer simulation of grain growth–I. Kinetics, Acta Metall. **32**, 783 (1984).

[28] C. Krill III and L.-Q. Chen, Computer simulation of 3-D grain growth using a phase-field model, Acta Mater. **50**, 3059 (2002).

[29] R. Perumal, P. K. Amos, M. Selzer, and B. Nestler, Phase-field study on the formation of first-neighbour topological clusters during the isotropic grain growth, Comput. Mater. Sci. **140**, 209 (2017).

[30] I. McKenna, S. Poulsen, E. M. Lauridsen, W. Ludwig, and P. W. Voorhees, Grain growth in four dimensions: A comparison between simulation and experiment, Acta Mater. **78**, 125 (2014).

[31] H. Ravash, J. Vleugels, and N. Moelans, Three-dimensional phase-field simulation of microstructural evolution in three-phase materials with different diffusivities, J. Mater. Sci. **49**, 7066 (2014).

[32] H. Ravash, J. Vleugels, and N. Moelans, Three-dimensional phase-field simulation of microstructural evolution in three-phase materials with different interfacial energies and different diffusivities, J. Mater. Sci. **52**, 13852 (2017).

[33] V. Yadav, L. Vanherpe, and N. Moelans, Effect of volume fractions on microstructure evolution in isotropic volume-conserved two-phase alloys: A phase-field study, Comput. Mater. Sci. **125**, 297 (2016).

[34] I. Ohnuma, K. Ishida, and T. Nishizawa, Computer simulation of grain growth in dual-phase structures, Philos. Mag. A **79**, 1131 (1999).

[35] D. Fan and L.-Q. Chen, Topological evolution during coupled grain growth and Ostwald ripening in volume-conserved 2-D two-phase polycrystals, Acta Mater. **45**, 4145 (1997).

[36] R. Perumal, P. K. Amos, M. Selzer, and B. Nestler, Phase-field study of the transient phenomena induced by 'abnormally' large grains during 2-dimensional isotropic grain growth, Comput. Mater. Sci. **147**, 227 (2018).

[37] P. Amos, Understanding the volume-diffusion governed shape-instabilities in metallic systems, arXiv:1906.10404.

[38] P. K. Amos and B. Nestler, Grand-potential based phase-field model for systems with interstitial sites, Sci. Rep. **10**, 22423 (2020).

[39] P. K. Amos and B. Nestler, Distinguishing interstitial and substitutional diffusion in grand-potential based phase-field model, Acta Mater. **12**, 100820 (2020).

[40] R. Perumal, M. Selzer, and B. Nestler, Concurrent grain growth and coarsening of two-phase microstructures; large scale phase-field study, Comput. Mater. Sci. **159**, 160 (2019).

[41] R. Perumal, P. K. Amos, M. Selzer, and B. Nestler, Quadrijunctions-stunted grain growth in duplex microstructure: a multiphase-field analysis, Scr. Mater. **182**, 16 (2020).

[42] P. K. Amos, R. Perumal, M. Selzer, and B. Nestler, Multiphase-field modelling of concurrent grain growth and coarsening in complex multicomponent systems, J. Mater. Sci. Technol. **45**, 215 (2020).

[43] P. W. Hoffrogge, A. Mukherjee, E. S. Nani, P. G. K. Amos, F. Wang, D. Schneider, and B. Nestler, Multiphase-field model for surface diffusion and attachment kinetics in the grand-potential framework, Phys. Rev. E **103**, 033307 (2021).

[44] N. Provatas and K. Elder, *Phase-Field Methods in Materials Science and Engineering* (Wiley, Hoboken, NJ, 2011).

[45] O. Tschukin, A. Silberzahn, M. Selzer, P. G. Amos, D. Schneider, and B. Nestler, Concepts of modeling surface energy anisotropy in phase-field approaches, Geotherm Energy **5**, 19 (2017).

[46] P. K. Amos, L. Mushongera, and B. Nestler, Phase-field analysis of volume-diffusion controlled shape-instabilities in metallic systems-I: 2-dimensional plate-like structures, Comput. Mater. Sci. **144**, 363 (2018).

[47] P. K. Amos, E. Schoof, D. Schneider, and B. Nestler, On the globularization of the shapes associated with alpha-precipitate of two phase titanium alloys: Insights from phase-field simulations, Acta Mater. **159**, 51 (2018).

[48] P. K. Amos, E. Schoof, J. Santoki, D. Schneider, and B. Nestler, Limitations of preserving volume in Allen-Cahn framework for microstructural analysis, Comput. Mater. Sci. **173**, 109388 (2020).

[49] M. Plapp, Unified derivation of phase-field models for alloy solidification from a grand-potential functional, Phys. Rev. E **84**, 031601 (2011).

[50] D. Fan, L.-Q. Chen, and S.-P. P. Chen, Numerical simulation of Zener pinning with growing second-phase particles, J. Am. Ceram. Soc. **81**, 526 (1998).

[51] S. O. Poulsen, P. Voorhees, and E. M. Lauridsen, Three-dimensional simulations of microstructural evolution in polycrystalline dual-phase materials with constant volume fractions, Acta Mater. **61**, 1220 (2013).

[52] T. Mittnacht, P. K. Amos, D. Schneider, and B. Nestler, Morphological stability of three-dimensional cementite rods in polycrystalline system: a phase-field analysis, J. Mater. Sci. Technol. **77**, 252 (2021).

[53] R. Ritasalo, M. Cura, X. Liu, Y. Ge, T. Kosonen, U. Kanerva, O. Söderberg, and S. Hannula, Microstructural and mechanical characteristics of Cu–Cu_2O composites compacted with pulsed electric current sintering and hot isostatic pressing, Composites Part A: Appl. Sci. Manufact. **45**, 61 (2013).

[54] S. Praveen, J. Basu, S. Kashyap, and R. S. Kottada, Exceptional resistance to grain growth in nanocrystalline CoCrFeNi high entropy alloy at high homologous temperatures, J. Alloys Compd. **662**, 361 (2016).

[55] M. Abadi, A. Agarwal, P. Barham, E. Brevdo, Z. Chen, C. Citro, G. S. Corrado, A. Davis, J. Dean, M. Devin, S. Ghemawat, I. Goodfellow, A. Harp, G. Irving, M. Isard, Y. Jia, R. Jozefowicz, L. Kaiser, M. Kudlur, J. Levenberg *et al.*, TENSORFLOW: Large-scale machine learning on heterogeneous systems (2016).

[56] A. Koeppe, Deep learning in the finite element method, Ph.D. thesis, RWTH Aachen University, Aachen, 2021.

[57] N. Brandt, L. Griem, C. Herrmann, E. Schoof, G. Tosato, Y. Zhao, P. Zschumme, and M. Selzer, Kadi4Mat: A research data infrastructure for materials science, Data Sci. J. **20**, 8 (2021).

[58] L. Li, K. Jamieson, G. DeSalvo, A. Rostamizadeh, and A. Talwalkar, Hyperband: A novel bandit-based approach to hyperparameter optimization, J. Mach. Learn. Res. **18**, 6765 (2017).

[59] D. Kingma and J. Ba, Adam: A method for stochastic optimization, arXiv:1412.6980.

[60] D.-H. Riu, Y.-M. Kong, and H.-E. Kim, Effect of Cr_2O_3 addition on microstructural evolution and mechanical properties of Al_2O_3, J. Eur. Ceram. Soc. **20**, 1475 (2000).

[61] D. Zhang, G. Weng, S. Gong, and D. Zhou, Computer simulation of grain growth of intermediate–and final-stage sintering and Ostwald ripening of $BaTiO_3$-based PTCR ceramics, Mater. Sci. Eng. B **99**, 428 (2003).

[62] B. Nestler, H. Garcke, and B. Stinner, Multicomponent alloy solidification: phase-field modeling and simulations, Phys. Rev. E **71**, 041609 (2005).